The Thesis Committee for Christopher Adam Griffith
Certifies that this is the approved version of the following thesis:

Analysis and Interpretation of a Hydraulic Fracture Treatment using Offset Vertical Observation Wells and a Hydraulic Fracture Simulator

APPROVED BY
SUPERVISING COMMITTEE:

Supervisor:

Mark W. McClure

David Nicolas Espinoza

Analysis and Interpretation of a Hydraulic Fracture Treatment using Offset Vertical Observation Wells and a Hydraulic Fracture Simulator

by

Christopher Adam Griffith, B.S. Ch.E.

Thesis

Presented to the Faculty of the Graduate School of

The University of Texas at Austin

in Partial Fulfillment

of the Requirements

for the Degree of

Master of Science in Engineering

The University of Texas at Austin

August 2015

Dedication

I dedicate this work to my parents

Acknowledgements

First and foremost, I want to thank my advisor Dr. Mark McClure for giving me the opportunity to work within his research group. During the past two years, I always enjoyed the ideas and insight that Mark provided. I'd like to say thank you for showing me what graduate research is all about and I appreciate the different angle you took when looking at new problems.

Thank you to Dr. Nicolas Espinoza for reading this work and for all the valuable feedback. Your comments made this piece stronger.

Thank you to Mrs. Frankie Hart for everything that you do for us graduate students. You make our lives so much easier.

I'd like to thank Sogo and Ming for making all the long hours that much more enjoyable. Good luck to the both of you.

Thank you to Statoil for providing the funding for this work.

I want to thank my parents for all the sacrifices they have made in their lives to make mine better and for always being supportive in my decisions. I also want to thank my two older brothers for keeping me in line but at the same time for not being too hard on me while growing up.

Lastly, I want to thank my wife for being supportive in my decision to pursue graduate school. Thank you for being patient with all the late nights, whether I was studying for tests or working on research, and thank you for all the little things you did to make my life a whole lot easier. I appreciate everything you do and I love you.

Abstract

Analysis and Interpretation of a Hydraulic Fracture Treatment using Offset Vertical Observation Wells and a Hydraulic Fracture Simulator

Christopher Adam Griffith, M.S.E.

The University of Texas at Austin, 2015

Supervisor: Mark W. McClure

Analysis of hydraulic fracture treatments requires incorporating a wide range of data in order to make useful inferences about fracture properties. For example, microseismic monitoring and production decline analysis can be used to obtain the hydraulic fracture half-length, which is an important parameter for field development. The challenge in using these tools is that the methods used for analysis are open to interpretation and can make it difficult to rely on the results.

This thesis integrates data from four horizontal wells that were hydraulically fractured in an unconventional shale play and results from a 2-dimensional hydraulic fracture simulator in order to make qualitative observations about fracture properties. The importance of the data set hinges on nine vertical observation wells that recorded pressure vs. time during the hydraulic fracture treatments. The observation wells were located at different distances and depths from the horizontal wells. This is important

because it removes some of the ambiguity associated with making interpretations from microseismic data, production decline analysis, or other methods.

Results from modeling and the data set indicated the following: (1) the networks of fractures created from these treatments were volumetric and complex, illustrated by the microseismic data and the pressure signals recorded at the observation wells, (2) microseismicity was generally successful in delineating where fluid progressed during pumping, (3) however, flow of fluid into fractures stimulated during previous stages was aseismic, a manifestation of the Kaiser effect, and (4) during long term production, fluid was not produced from the more distant parts of the reservoir that were pressurized and stimulated during the fracturing treatment.

To explain these four observations, we hypothesize that proppant was not transported to the regions of the stimulated rock volume that were most distant from the stimulated wells. The stimulated, but unpropped, fractures in this region evidently lost much of their conductivity after closure that they did not contribute significantly to long term production.

Table of Contents

List of Tables

List of Figures

Chapter 1: *Introduction*

Since the early 1970s, the United States daily production of crude oil has steadily declined. However, in the mid-2000s, this trend was revered due in large part to increased production from unconventional formations. The primary factors driving the increased production were favorable economic conditions (Montgomery et al., 2005) and improvements in drilling and completion practices (Warpinski et al., 2013; Browning et al., 2013). Currently, the production of crude oil from unconventional formations accounts for approximately 4 of the 92 million barrels of oil produced per day globally (US EIA, 2015).

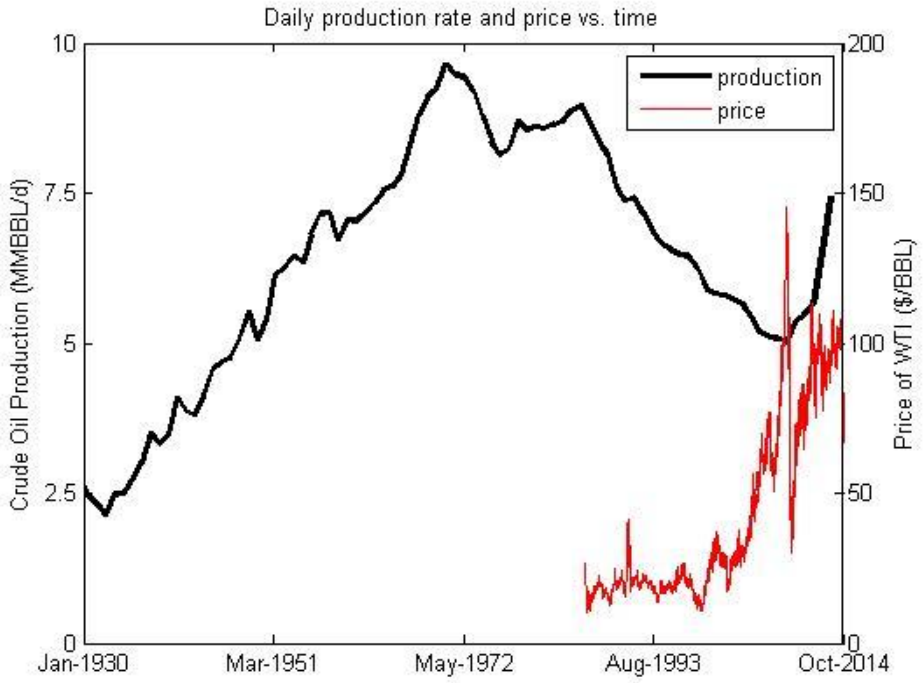

Figure 1 – United States daily oil production in millions of barrels per day and price of oil ($/barrel). Data is from United States Energy Information (USEIA).

The United States, along with many other countries in the world, sits atop vast reserves of both crude oil and natural gas (Figure 2 and Figure 3). However, these reserves are mostly trapped in unconventional shale oil (tight oil) or shale gas (tight gas) reservoirs. Shale is characterized as fine-grained sedimentary rock that contains pore throats on the nanometer to micrometer range (Shrock, 1946). The small pore throats are responsible for the nano to micro darcy permeabilities typically observed in shale formations, and because of the low permeabilities, these formations cannot be produced without some mechanism of stimulation.

Rank	Country	Shale oil (billion barrels)	
1	Russia	75	
2	U.S. [1]	58	(48)
3	China	32	
4	Argentina	27	
5	Libya	26	
6	Australia	18	
7	Venezuela	13	
8	Mexico	13	
9	Pakistan	9	
10	Canada	9	
	World Total	**345**	**(335)**

[1] EIA estimates used for ranking order. ARI estimates in parentheses.

Figure 2 – Top 10 countries with technically recoverable shale oil resources. Information from US EIA (http://www.eia.gov/analysis/studies/worldshalegas/)

Rank	Country	Shale gas (trillion cubic feet)	
1	China	1,115	
2	Argentina	802	
3	Algeria	707	
4	U.S.[1]	665	(1,161)
5	Canada	573	
6	Mexico	545	
7	Australia	437	
8	South Africa	390	
9	Russia	285	
10	Brazil	245	
	World Total	**7,299**	**(7,795)**

[1] EIA estimates used for ranking order. ARI estimates in parentheses.

Figure 3 – Top 10 countries with technically recoverable shale gas resources. Information from US EIA (http://www.eia.gov/analysis/studies/worldshalegas/)

Hydraulic fracturing is one of the key technologies that has allowed for the extraction of oil and gas from unconventional formations. Hydraulic fracturing is a stimulation technique used to enhance fluid flow in low permeability rock. The improved fluid flow is achieved by isolating sections of the wellbore with the aid of packers, followed by pumping fluid into the wellbore at high pressures (Hubbert, 1972; Warpinski, 2013). The fluid is pumped at pressures higher than the minimum stresses acting on the formation, such that a network of fractures and fissures are created (Hubbert, 1972). Included in the stimulation fluid are small particles referred to as proppant. The proppant particles are small enough to be transported within the newly created hydraulic fractures, and they are strong enough so that once fluid injection has stopped, the fractures are "propped" open indefinitely. The result is highly permeable

pathways that allow for oil and gas to flow more freely to the wellbore. The increased fluid flow allows for commercial volumes of hydrocarbons to be extracted at an economic rate.

Advances in horizontal drilling have also played a large role in the improved recovery of hydrocarbons from unconventional formations. The main idea behind horizontal drilling is to drill a vertical portion of a well to a targeted depth, deviate horizontally, and then continue to drill a lateral portion of the well. The long lateral section increases the contact area between the wellbore and formation (increasing production from a single well) and decreasing the total number of wells required producing hydrocarbons (McClure, 2012; Vincent, 2012; Warpinsk et al., 2013).

The technologies of hydraulic fracturing and horizontal drilling have been an enormous engineering success. However, even with their success, there are still opportunities to optimize aspects of the treatment process. In the past several years, research has been focused on answering fundamental questions such as: (1) How far fluid progress during stimulation (e.g., what is the fracture half-length), and what portion of the fractures actually contributes to production (Barree et al., 2005; Cipolla et al., 2008; Vincent, 2012)? (2) How well do microseismic events correlate with fluid progression from hydraulic fracturing? And (3) how do newly created hydraulic fractures interact with preexisting natural fractures, and what impact does this interaction have on the stimulated fracture network and overall production?

1.1 Research Overview

The focus of this work was to make use of a unique field data set. The data set included a full suite of information (surface injection pressure, microseismic data, injection rate, etc.) from four horizontal wells that were hydraulically fractured in a US unconventional shale play. The uniqueness of the data stems from the vertical observation wells that were scattered throughout the field. The observation wells had pressure and temperature sensors that allowed for discrete measurements to be recorded during stimulation and subsequent production. This is important because it removes some of the ambiguity associated with traditional indirect measurement techniques that are used in evaluating hydraulic fracture treatments (e.g., advanced pressure decline analysis or microseismic observations).

The data from the observation wells enabled us to formulate general questions with regard to the hydraulic fracturing process. Some of these were: how well does the observed fluid progression from the microseismic data correlate to the pressure trends at the vertical wells? (e.g., what is the hydraulic fracture half-length), what portion of the hydraulic fractures are actually contributing to production? Did we see evidence of fracture complexity from the pressure trends in the observation wells? Did the different stimulated formation layers have the same pressure trends? Where were the vertical wells located in relation to the created hydraulic fracture network? Are there different mechanisms that can create hydraulic connection between the vertical observation wells

and the stimulation wells? Does the nature of the hydraulic connection impact future production from that portion of the reservoir?

After completing a general analysis of the field data, the next step was to calibrate a numerical hydraulic fracture simulator. The simulator used for this research was CRFAC, which stands for Complex Fracture ReseArch Code. The code was developed by McClure and Horne (2013). Model calibration was performed based on the observed initial shut-in pressure and the size of the region of microseismicity created by each stage. In addition, we attempted to match the far field pressure at the observation wells from our simulation results to the field data. The goal of our modeling was to simulate qualitatively all of the pressure trends that were observed at the observation wells. The simulator had success at matching some of the trends, but not all.

1.2 Literature Review

With the increased use of hydraulic fracturing in the last ten years, considerable effort has been focused on understanding the basic physical processes that take place during stimulation of unconventional formations. The goal is to incorporate our knowledge and understanding of the process into computational models in order to optimize stimulation treatments.

One aspect of modeling that has received significant attention is the idea that hydraulic fractures in unconventional formations create volumetric and complex features/networks (Barree et al., 2005; Cipolla et al., 2008; McClure, 2012; Vincent, 2012; Warpinsk et al., 2013; Manchanda et al., 2014; Taleghani and Olson, 2014; Downie et al., 2015). The challenges in determining how far these volumetric, complex fracture networks propagate during a treatment and how they contribute to the overall production of a formation are numerous, and will be described below.

From a design engineer's point of view, understanding how and why complex fractures form is important because it has a significant impact on how a stimulation treatment should be designed and how a field will be developed (Barree et al., 2005; Cipolla et al., 2008; McClure, 2012; Vincent, 2012; Warpinsk et al., 2013; Manchanda et al., 2014; Taleghani and Olson, 2014; Downie et al., 2015). Being able to predict whether or not a fracture is volumetric (and complex) can be advantageous because it could prevent the unnecessary stimulation of a formation that would be more conducive to a conventional, planar fracture feature (Warpinski, 2008; Manchanda et al., 2014). In

addition, being able to determine the spatial extent to which fractures propagate is important because it is one of the primary drivers in establishing how far (or close) adjacent horizontal wells should be placed during field development (Warpinski, 2008). Inaccurate estimates of the hydraulic fracture half-length can negatively impact field development by: (1) yielding lower than expected hydrocarbon recovery, (2) result in costly "modifications to fracture treatments" (Cipolla et al., 2008), and (3) potentially result in infill drilling for increased hydrocarbon recovery.

Further highlighting the importance of establishing an appropriate hydraulic fracture half-length, companies producing from unconventional formations are continually seeking to streamline drilling and completion processes (Arguijo et al., 2012). In general, the basic goal of streamlining is to develop one (or several) stimulation treatments and use the same process on all wells within a given field. The benefit for companies is they can better control costs associated with fracturing a well. Costs are better controlled by focusing on one (or several) treatments as opposed to performing a wide range of treatment schedules. The downside however, is that one (or a few) fracture treatment designs will not necessarily be the most effective for extracting hydrocarbons from a shale field.

We would like to be able answer the following questions: (1) based on geologic conditions (principal stress magnitudes and directions, rock type, etc.) and engineered stimulation parameters (e.g., injection fluid, injection rate, injection pressure, stage spacing, cluster spacing, etc.), how far will hydraulic fractures propagate? (2) What portion of these hydraulic fractures will contribute to production? The general

observation in the literature has been the distance of fluid progression during stimulation (e.g., the hydraulic fracture half-length) is greater than the length of a hydraulic fracture that contributes to production (e.g., the effective hydraulic fracture half-length) (Barree et al., 2005; Cipolla et al., 2008; Manchanda et al., 2014). One possible explanation for this observation is that our general understanding of how fluid and proppant interact during stimulation is still relatively incomplete (Barree et al., 2005; Cipolla et al., 2008).

Determining the hydraulic fracture half-length and the producing length of a hydraulic fracture is challenging for a variety of reasons, but the most obvious challenge is that hydraulic fracturing occurs deep within the earth, and because of this, it is difficult (if not impossible) to observe directly what is going on (Cipolla et al., 2008; McClure, 2012; Warpinski et al., 2013). In addition, shale formations contain both preexisting natural fractures and bedding planes, making it difficult to predict how newly created hydraulic fractures will interact with these discontinuities during stimulation (Cipolla et al., 2008; Cipolla et al., 2008; McClure, 2012; Manchanda et al., 2014; Taleghani and Olson, 2014; Downie et al., 2015).

The combination of problems that: (1) we cannot directly observe hydraulic fracturing (and the fracturing we have been able to observe is highly limited) (Warpinksi and Teufel, 1987), and (2) we have an incomplete understanding of the interaction between newly created fractures and preexisting fractures, makes it challenging to answer fundamental questions about the underlying physics that take place during stimulation. As a result, differing philosophies exist on what exactly creates fracture complexity.

There are several concepts found within the literature that describe how volumetric fractures are created. One of these concepts is that a single primary fracture forms, with leakoff into secondary fractures that are either opened by injection or induced to fail from shearing (Figure 4) (Warpinski et al., 2001; Palmer et al., 2007; Rogers et al., 2010; Nagel et al., 2011; Roussel and Sharma, 2011; McClure and Horne, 2013). Another concept is that the fracture network branches because propagating fractures terminate against preexisting fractures and other preexisting planes of weakness (Damjanac et al., 2010; Weng et al., 2011; Wu et al., 2012; McClure and Horne, 2013). Because we cannot observe hydraulic fracturing, there is not unanimous agreement on the mechanisms that contribute to fracture complexity.

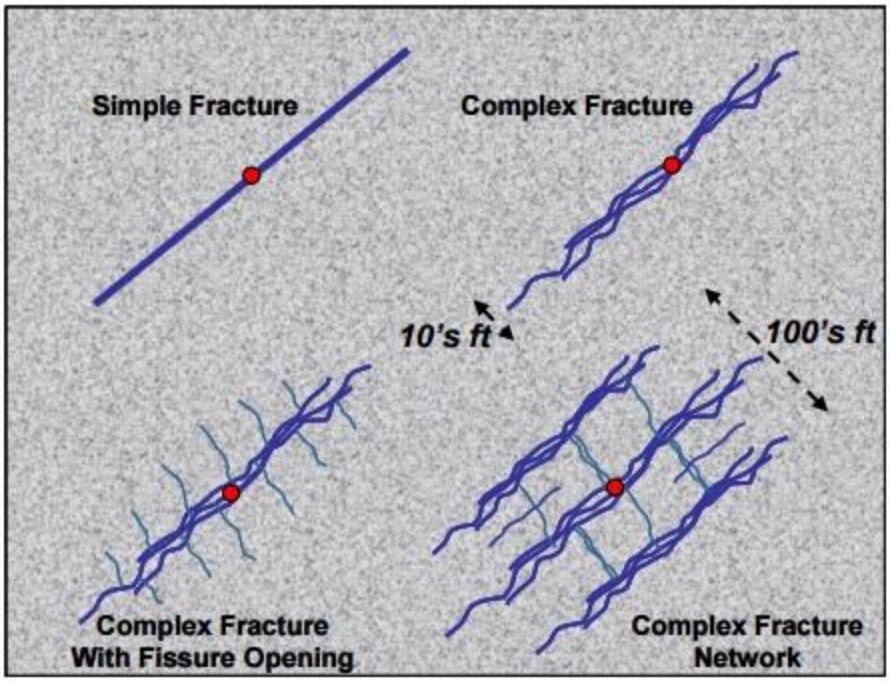

Figure 4 – A graphical description of simple fracture features, complex fractures, complex fractures with fissure opening, and complex fracture network. Image from Cipolla et al. (2008).

A variety of methods are available to estimate the hydraulic fracture half-length and effective hydraulic fracture half-length. Some of the common methods available to estimate fracture half-length are: production decline analysis, pressure transient analysis, fracture modeling, microseismic and tiltmeter data, and numerical reservoir modeling (Barree et al., 2005; Cipolla et al., 2008; Warpinski et al., 2013). Each of the different methods has their unique advantages and disadvantages. However, they all have one major disadvantage because they indirectly estimate properties of hydraulic fractures.

For example, a common method used to estimate the effective hydraulic fracture half-length is production decline analysis. The basic concept is to assume a fracture geometry (usually a planar feature) and to perform an "iterative process that couples

material balance (calculations), decline curves, and traditional pressure transient techniques" (Barree et al., 2005). This iterative process is highly nonunique, sensitive to model assumptions and as a result, makes it difficult to rely on solutions without some method of calibration (Cipolla et al., 2008). In addition, filtering production data can be a highly intensive and non-straightforward process that introduces more uncertainty and error in calculated properties (Downie et al., 2015). These methods can provide some useful results, such as reasonable predictions of future production, but cannot be relied upon to give detailed insight into the nature of the fracture network.

Another common method used to measure the fracture half-length is microseismic monitoring (Warpinksi et al., 2013). Microseismic monitoring is a tool used to detect the fracture half-length by observing the energy released from small shear slip events during hydraulic fracturing (Warpinsiki et al., 2009). Geophone arrays are placed at the surface or within offset wells that are near and at similar depth as the stimulated interval. The placement of the arrays can greatly impact the data that is collected (Warpinski et al., 2009). The receivers allow for the microseismic events to be indirectly monitored and tracked by using geophysical (acoustic) models that assume rock properties in order predict P- and S-wave velocities. The P- and S-wave velocities are then used to calculate the arrival time to the geophone array which then allow for the location a microseismic event to be determined (Warpinski et al., 2009). It is often assumed that wherever there has been a recorded microseismc event, there has been fluid invasion of that particular area, though this is not necessarily the case (Huang et al., 2014).

Microseismic monitoring has several major advantages over other methods used to predict the hydraulic fracture half-length. The primary advantage is that microseismic monitoring works in real time. Real time monitoring allows for the operator to observe where fluid progression extends during a fracture treatment and make adjustments on-the-fly to potentially improve the treatment. Another advantage is that microseismic monitoring allows for the operator to determine whether or not the created stimulated region is complex. Understanding stimulation complexity can impact stimulation design and well placement.

Typical analysis of a stimulation treatment utilizes some combination of microseismic data, production decline analysis, and surface injection pressure data in order to make evaluations about the fracture treatment. Production decline analysis requires good production data, which can take years to obtain and properly filter. Downie et al. (2015) point out that a method that uses microseismic data and surface injection pressure has several deficiencies and can also lead to inaccurate estimates of fracture properties because of "variability of fluid friction, slurry density, perforation restrictions, and other near-wellbore pressures when computing bottom hole fracturing pressure."

Barree et al. (2005) highlight the discrepancies from the different methods used for predicting the hydraulic fracture half-length and effective hydraulic fracture half length. In his analysis, an estimated hydraulic fracture half-length determined from a fracture model varied as much as 74.7% when compared to the half-length obtained from pressure transient analysis. He shows that fracture estimates from an un-calibrated

fracture simulator produced an estimate of the hydraulic fracture half-length that differed by as much as 96.9% when compared to results obtained from microseismic and production decline analysis results (Barree et al., 2005).

Obtaining an accurate representation of an effective hydraulic fracture half-length is an important step in improving our efficiency in extracting hydrocarbons from unconventional reservoirs. The common pitfalls with current methods are they infer hydraulic fracture properties indirectly. While costly to implement, direct methods for measuring fracture properties should occasionally be implemented to help constrain critical parameters that can have a positive impact on improved hydrocarbon recovery. By calibrating models with direct measurements, we can improve our ability to create optimal fracture treatments and improve the efficacy of hydraulic fracture simulation models.

Chapter 2: *Field Data*

Chapter 2 introduces the field data set used in this study. It first introduces the available data, and discusses general information about the horizontal wells such as how they were stimulated, and other supplementary information. It then discusses in general terms the trends that were observed at the observation wells. Lastly, a more detailed discussion of the short term pressure responses (during hydraulic fracturing) and long term pressure responses (during production) is provided.

2.1 Description of the data set

The information provided by the company included data for four hydraulically fractured horizontal wells in an unconventional shale reservoir. The average reservoir porosity was 8-12%. The formation permeability (from the GRI method using crushed shale samples) was estimated to be in the range of 0.14 nD – 2,256 nD depending on the formation layer. Diagnostic fracture injection tests provided an upper bound permeability of 66 μD.

There were a total of 8 formation layers. Three of the layers were targeted for hydrocarbon production (Layers 1, 2, and 3) and it is likely the other formation layers also contributed to production. The average thickness of each layer was approximately 35.6 ft. Details of the formation layers are provided in Table 1.

Table 1 - Average thickness of formation layers

Layer Name	Approximate Thickness (ft.)	Approximate Thickness (m)	GRI Perm (nD)	DFIT Perm (nD)
Layer A	22.6	6.9	3.43	
Layer 1	50.7	15.5	34.54	66000
Layer B	32.1	9.8	2.57	
Layer 2	38.4	11.7	30.40	4000
Layer C	38.4	11.7	8.32	
Layer D	59.4	18.1	0.14	
Layer E	24.4	7.4	0.60	
Layer 3	19	5.8	2255.77	
Total	285	86.9		
Avg Thickness	35.6	10.9		

For each of the hydraulic fracture treatments, the number of stages, the injection rate, the volume of proppant per stage, the total volume of slurry per stage, and other design parameters were similar. The formation minimum principal stress was estimated to be 5,510 psi (38 MPa), based on DFIT tests performed by a service company.

The wells were stimulated sequentially such that all stages within each well were fractured before stimulation of the next well. The four wells were stimulated over a period of ten days. Well 1 required about two days for stimulation. Wells 2, 3, and 4 required about 30 to 40 hours each. Well 1 required more time for stimulation because of operational issues. The wells were stimulated in the following order: 1,2,3,4 (Figure 5).

The wells were drilled to a true vertical depth of 7,300 ft. (2,225 m) and each well had an average lateral length of 4,000 ft. (1,219 m). Well spacing ranged from 750 ft. – 1,050 ft. (228.6 m – 320 m) The wells were completed with 20 stages (except for well 1, which had 19 stages). The average length of each stage was 195 ft. (59.4 m). This stage spacing was consistent between all of the wells.

The wells were stimulated with an average of 1.6 million gallons of water (6060 m^3) and 3.4 million pounds (1.54 million kg) of total proppant (distributed evenly among the stages). The average injection rate for the stimulation treatment was 55 barrels per minute (143 l/s) and each stage was fractured for roughly one hour.

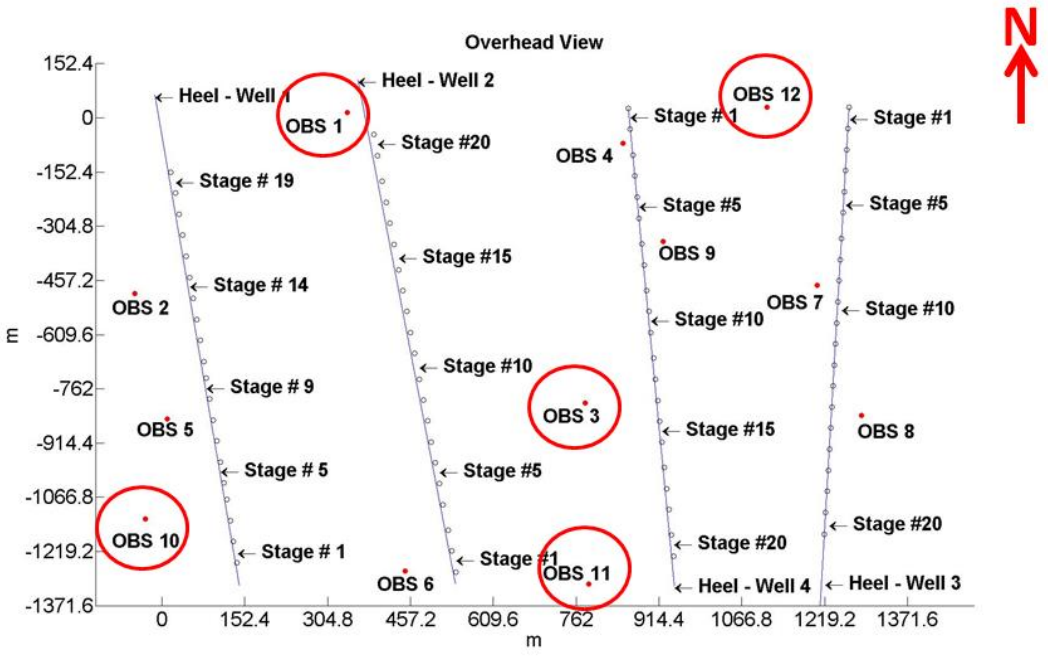

Figure 5 – Overhead view of the 4 horizontal wells. The red dots in the plot represent the location of the vertical observation wells. The large red circles show which observation wells were equipped with microseismic monitoring equipment. The plot also includes the location of stages for each of the horizontal wells. The heel of wells 1 and 2 are on the northern part of the plot whereas the heel of wells 3 and 4 are on the southern part of the plot.

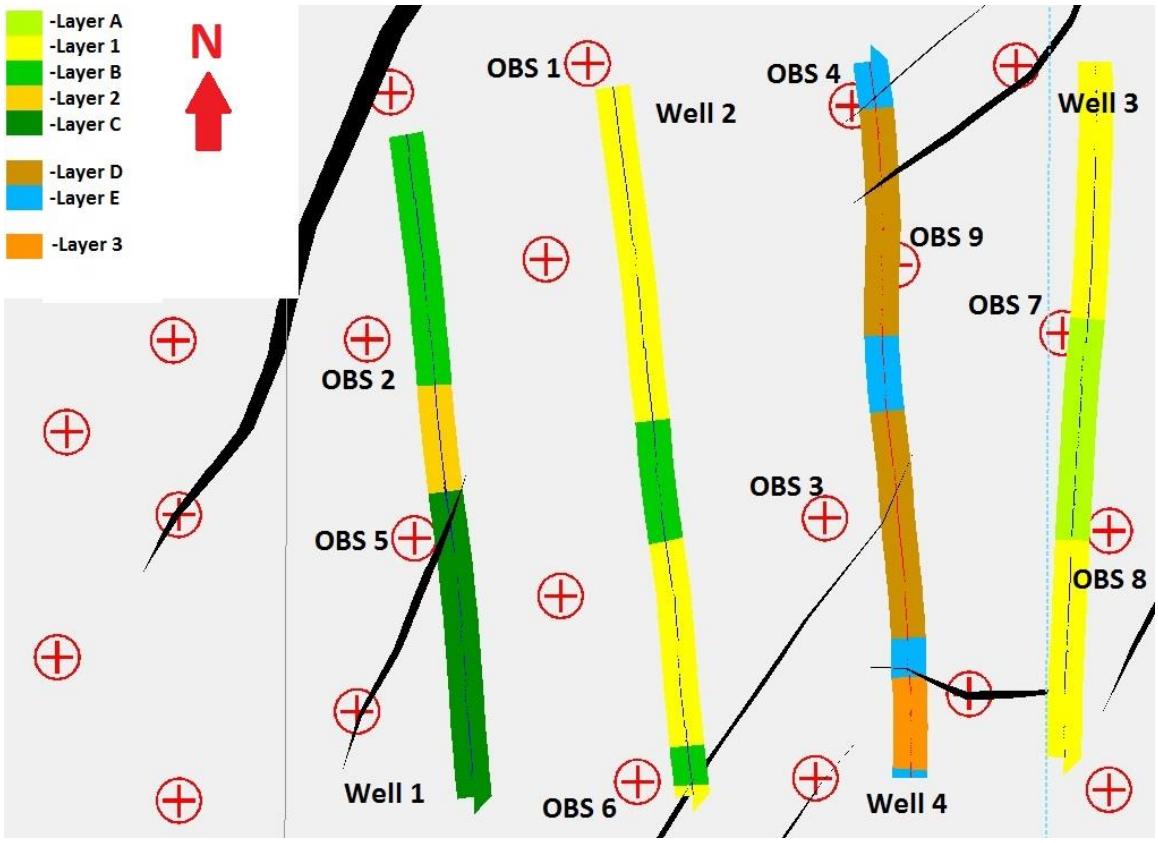

Figure 6 – Overhead view of the 4 horizontal wells and the formation layers they were landed in.

Table 2 - Percentage of formation layer each of the 4 wells were landed in

	Well 1	Well 2	Well 3	Well 4
Layer A	-	-	40%	-
Layer 1	-	80%	60%	-
Layer B	40%	20%	-	-
Layer 2	15%	-	-	-
Layer C	45%	-	-	-
Layer D	-	-	-	65%
Layer E	-	-	-	20%
Layer 3	-	-	-	15%

Ten years prior to hydraulically fracturing the horizontal wells, nine vertical wells had been drilled and hydraulically fractured in the formation. The wells were produced

for approximately ten years, after which the wells were shut in and installed with pressure and temperature sensors at different depths. Information about how the vertical wells were previously hydraulically fractured in addition to their production rates was unavailable to us.

Observation wells 1, 3, 10, 11, and 12 were used to record microseismic data during hydraulic fracturing. Because these wells recorded microseismic events, they were unable to record pressure vs. time data during hydraulic fracturing. Observation wells 3 and 11 recorded microseismic data during stimulation of all four horizontal wells. Observation wells 1 and 10 recorded microseismic during stimulation of horizontal wells 1 and 2 and observation well 12 recorded microseismic during stimulation of horizontal wells 3 and 4.

The key aspect of this data set is the pressure and temperature measurements that were recorded from the offset vertical observation wells. This information, which is not usually available, was valuable because it allowed for observations of pressure behavior in the far-field, away from the hydraulically fractured wells.

Because the pressure gauges were located at different depths within the formation, they allowed for the investigation of vertical connectivity between the different targeted layers. Interpreting vertical connectivity between different formation layers is difficult when only using microseismic data or other methods for fracture interpretation.

Integrating the microseismic data with the pressure data at the injection and observations wells allowed us to make useful inferences about: (1) how far fluid progressed during stimulation, (2) what portion of the hydraulic fractures contributed to

production (e.g., the effective hydraulic fracture half-length), (3) the fracture geometry created from stimulation, (4) vertical connectivity between the different reservoir layers being stimulated, and (5) the location of the created hydraulic fracture network with respect to the vertical wells.

Because of the large volume of data contained within the data set, a general work flow was developed to help focus our efforts. The work flow was:

1. Gather and consolidate applicable files from the data set.
2. Create MATLAB files to integrate various parts of the data set for interpretation.
3. Create MATLAB videos that allow us to view (in real time): injection pressure vs. time of the horizontal wells, pressure vs. time in the offset vertical observation wells, along with an overhead view of the field that includes the creation of microseismic events during stimulation.
4. Interpret the pressure trends at the different vertical observation wells (both short term and long term pressure trends).
5. Categorize the wells based on the qualitative behavior of the pressure trends at the observation wells.
6. Establish general hydraulic fracture half-lengths from the data set by comparing pressure responses at the observation wells to the microseismic data that was available.
7. Develop a set of working hypotheses to explain the different types of pressure trends at the observation wells.

8. Simulate the hypothesized scenarios using a numerical hydraulic fracture simulator (CFRAC). The goal was not to match the data exactly, but to see if the same general trends could be created. Data available from the data set (e.g., injection rate, formation minimum horizontal stress) were used in the simulations.
9. Compare the simulation results to the field data to evaluate the suitability of the hypothesized mechanisms.

2.2 General description of pressure response data:

There were a total of nine vertical observation wells that recorded pressure vs. time data in the data set. Only seven of the nine wells recorded pressure vs. time data during stimulation of the horizontal wells. The other two wells (observation wells 1 and 3) were used to acquire microseismic data during stimulation. Long term pressure vs. time data is available for all wells except observation well 1.

Table 3 – General information about the nine vertical observation wells.

Observation Well #	Active during stimulation	Closest Horizontal Well	Distance from Closest Horizontal Well (ft.)	Distance from Closest Horizontal Well (m)
1	NO	Well 2	100	30.5
2	YES	Well 1	370	112.8
3	NO	Well 4	435	132.6
4	YES	Well 4	50	15.2
5	YES	Well 1	170	51.8
6	YES	Well 2	300	91.4
7	YES	Well 3	140	42.7
8	YES	Well 3	215	65.5
9	YES	Well 4	100	30.5

The total duration of the recorded data spanned approximately 18 months. We decided to subdivide the pressure vs. time data into two groups. The first group was classified as short term pressure responses. The short term pressure responses were pressure responses that occurred during hydraulic fracturing of the horizontal wells (generally 2 days of total data). The second group was classified as long term pressure responses. The long term pressure response group consisted of data that was collected during the entire 18 months that data was recorded.

Based on the pressure behavior, the short term pressure responses were categorized into four groups. The four short term pressure response groups/trends were:

1. A large and rapid pressure increase that was above the formation minimum principal stress, followed by a pressure decrease.
2. A large and rapid pressure increase, below the formation minimum principal stress, followed by a pressure decrease (rapid or gradual).
3. A slow and continuous pressure increase, below the minimum principal stress.
4. A very slight (less than 14 psi (0.096 MPa)) pressure response.

Short Term Pressure Response Trend 1:

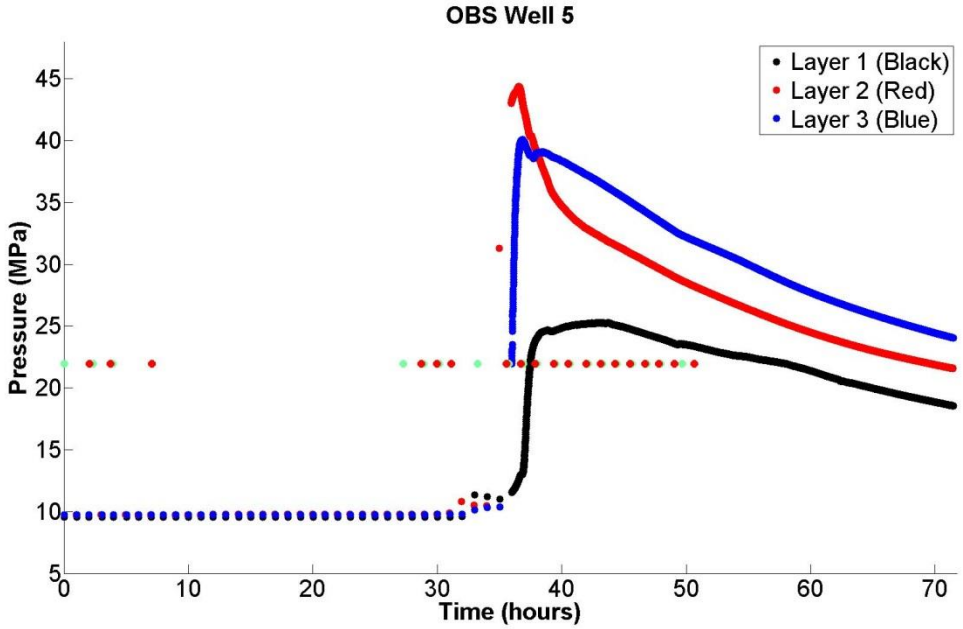

Figure 7 – Observation well 5, located to the left of horizontal well 1. Green dots represent the start of stimulation for a stage. Red dots represent when stimulation of a stage was completed. The black line represents layer 1 (shallowest), the red line represents layer 2, and the blue line represents layer 3 (deepest).

Short Term Pressure Response Trend 2:

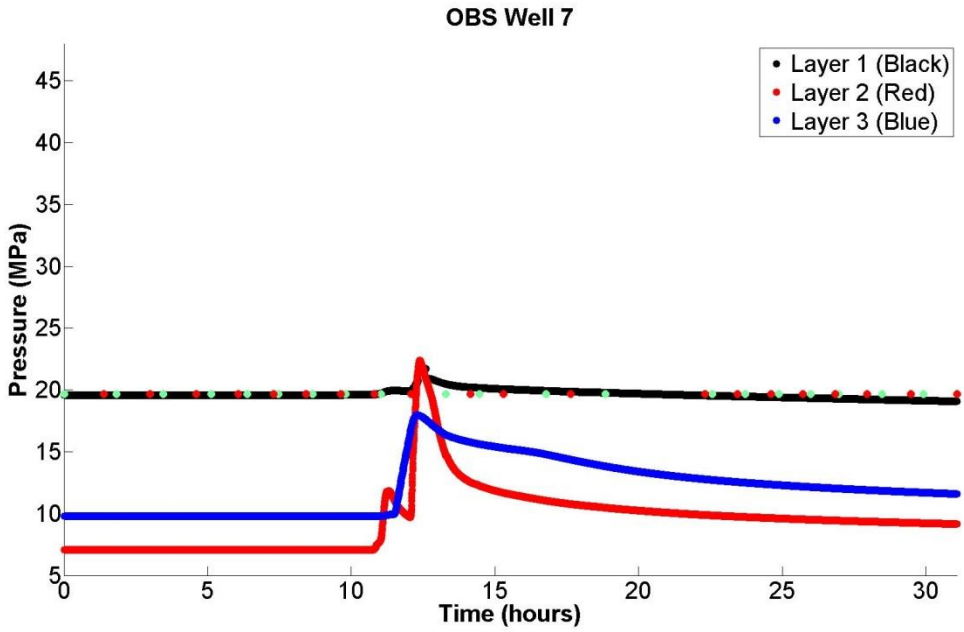

Figure 8 - Observation well 7, located to the left of horizontal well 3. Green dots represent the start of stimulation for a stage. Red dots represent when stimulation of a stage was completed. The black line represents layer 1 (shallowest), the red line represents layer 2, and the blue line represents layer 3 (deepest).

Short Term Pressure Response Trend 3:

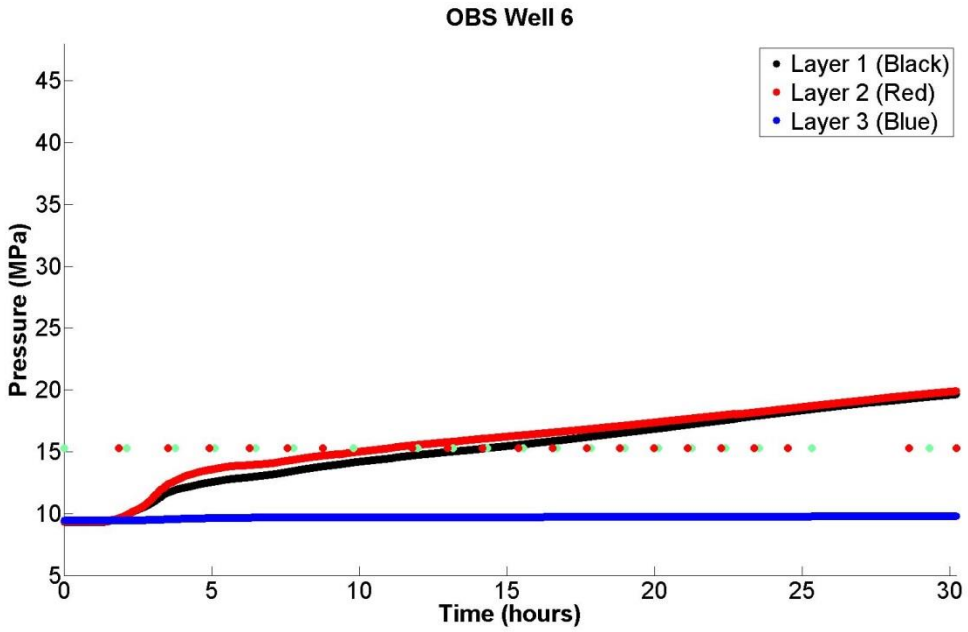

Figure 9 - Observation well 6, located to the left of horizontal well 2. Green dots represent the start of stimulation for a stage. Red dots represent when stimulation of a stage was completed. The black line represents layer 1 (shallowest), the red line represents layer 2, and the blue line represents layer 3 (deepest).

Short Term Pressure Response Trend 4:

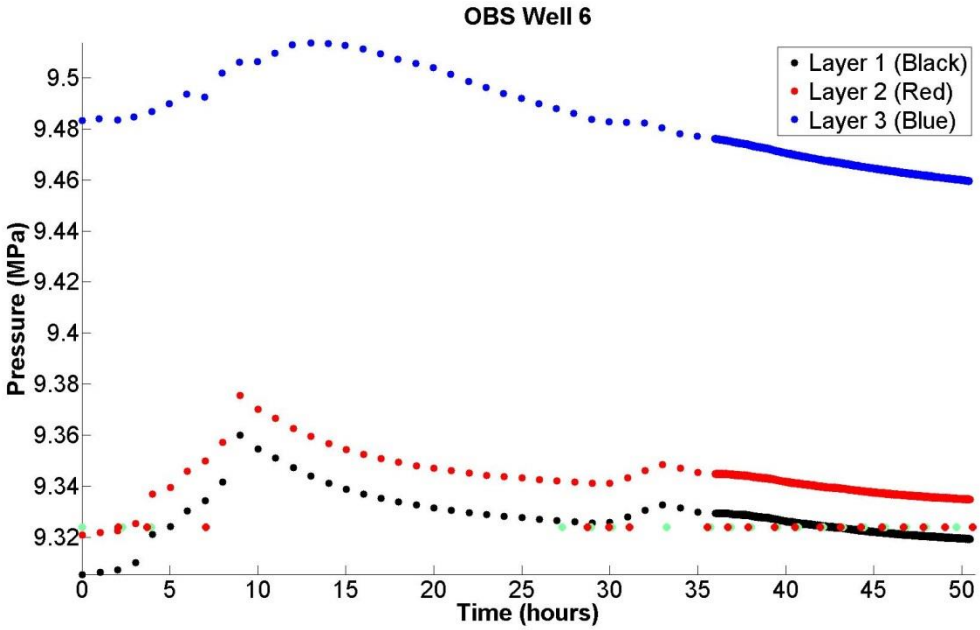

Figure 10 - Observation well 6, located 1,000 ft. (304.8 m) to the right of horizontal well 1. Green dots represent the start of stimulation for a stage. Red dots represent when stimulation of a stage was completed. The black line represents layer 1 (shallowest), the red line represents layer 2, and the blue line represents layer 3 (deepest). This plot represents a poroelastic pressure response during stimulation of well 1.

Prior to analyzing the data, it was hypothesized that poroelastic pressure responses due to the stresses induced by fracturing would be clearly visible. This was expected because the opening and propagation of hydraulic fractures in a formation generates stresses and strains in the surrounding rock matrix. These stresses and strains would presumably extend further into the formation than stimulation fluid from hydraulic fracturing. However, in this dataset, poroelastic pressure responses were generally not

observed. In one well, a very modest poroelastic response was observed (Figure 10). In the other wells, there were no signs of poroelastic pressure responses.

After investigating the properties of the formation fluid, it was determined that poroelastic pressure responses at the observation wells were minimal because of the large compressibility of the formation fluid. The reservoir fluid is a volatile oil, and the reservoir pressure was well below the fluid bubble point pressure. As a result, the reservoir fluid must have a very high compressibility, probably on the order of 10^{-3} psi^{-1} (0.145 MPa^{-1}) and possibly higher. Very high fluid compressibility will lead to very small poroelastic pressure response because the fluid requires minimal pressure change to accommodate volumetric strain.

An example to conceptually illustrate the idea of a poroelastic pressure response can be shown using Figure 11. In Figure 11, well 1 is adjacent to a propagating hydraulic fracture (in red). If the compressibility of the formation fluid is low, then well 1 would in theory record a pressure response induced from the stresses created from the propagating hydraulic fracture. Fluids with a low compressibility (e.g., oil above its bubble point) require a large pressure change to accommodate a small volumetric strain. If however the fluid compressibility of the formation fluid was very high, the poroelastic pressure

response would be minimal.

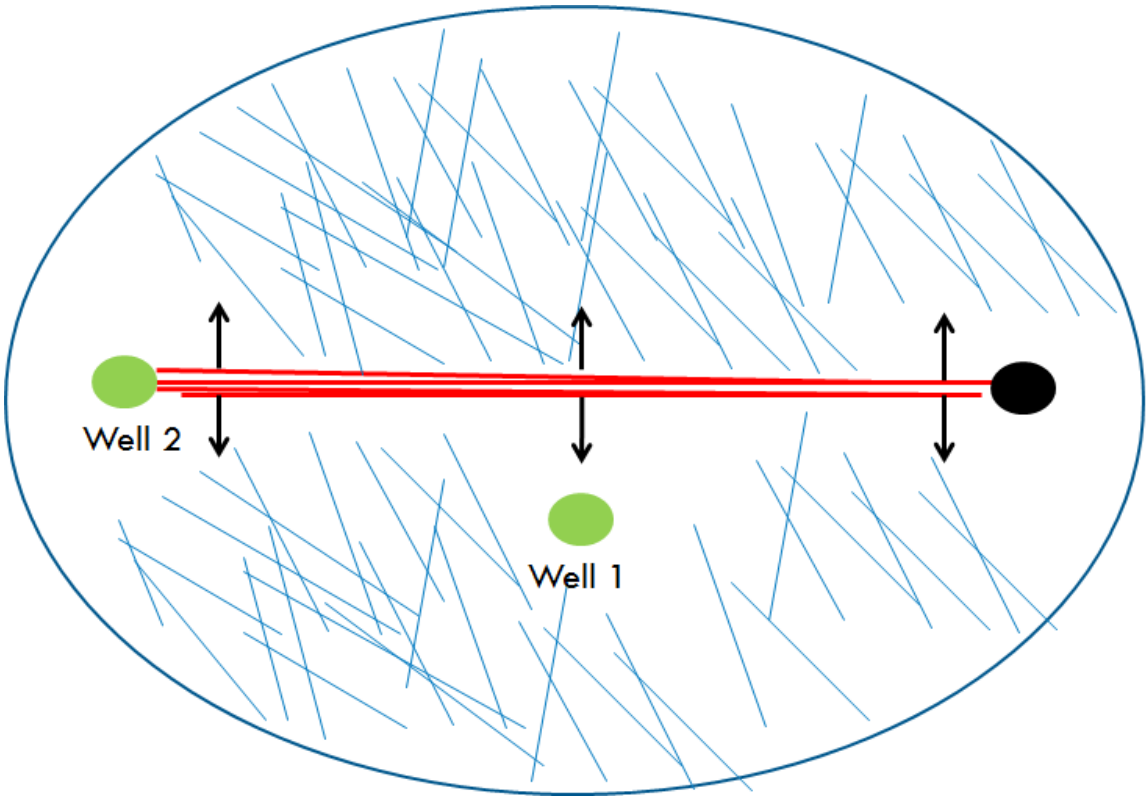

Figure 11 – Schematic of a hydraulic fracture (in red) propagating away from an injection well (in black) and intersecting observation well 2 (green) with stresses induced from fracturing interacting with observation well 1. The blue lines in the figure represent natural fractures in the formation.

Therefore, we believe that the pressure responses that were observed in the data were due to direct hydraulic connection between the injection well and the observation wells. Because the observation wells were previously fractured, it was easier for the newly forming hydraulic fractures to intersect them. Furthermore, because they had been produced, they were in a region of depleted pressure, and therefore lower stress, which would encourage newly forming fractures to propagate towards them.

The long term pressure responses were categorized into three groups/trends. The long term pressure responses all had an initial up-down pressure signal during stimulation of the neighboring horizontal well, followed by a different signal for each of the three groups. The three trends were:

1. An initial pressure increase (caused by the hydraulic fracturing), followed by a long term pressure decrease. This was referred to as an UP-DOWN trend.
2. An initial pressure increase followed by a pressure decrease. After the pressure decrease there was another pressure increase followed by a pressure decrease. This was referred to as an UP-DOWN-UP-DOWN trend.
3. An initial pressure increase after which there was a small decline in pressure. The pressure decrease was followed with a pressure increase/plateau. This was referred to an UP-DOWN-UP trend.

Long Term Pressure Response Trend 1:

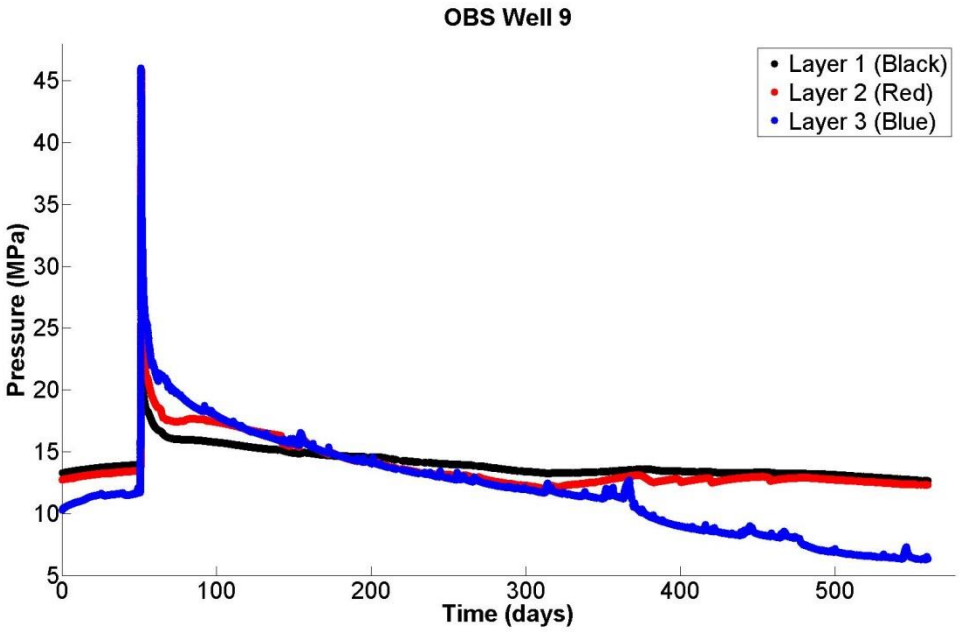

Figure 12 - Observation well 9, located to the right of horizontal well 4. The black line represents layer 1 (shallowest), the red line represents layer 2, and the blue line represents layer 3 (deepest). The plot also includes pressure buildup 40 days prior to hydraulic fracturing.

Long Term Pressure Response Trend 2:

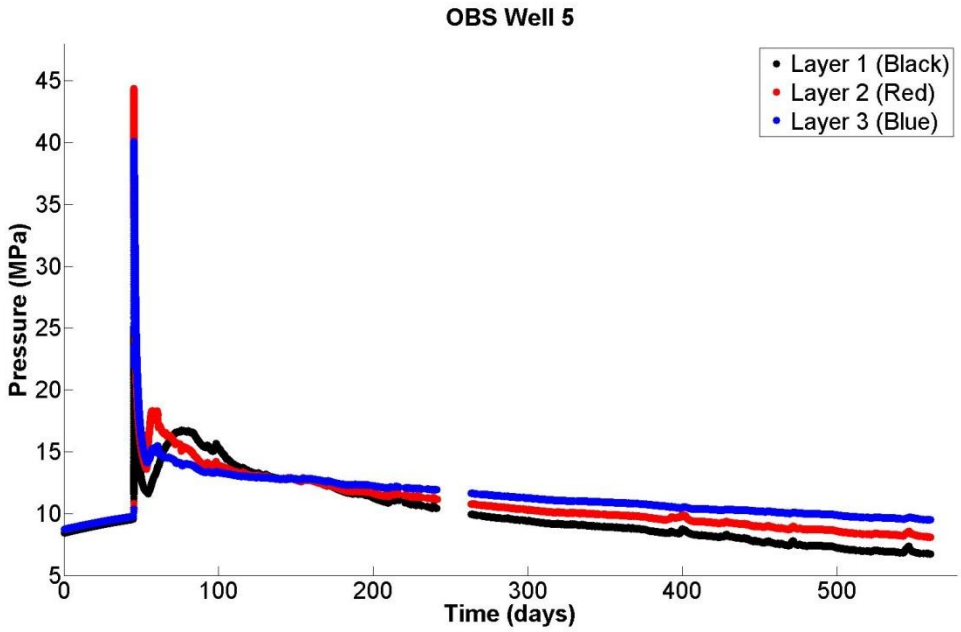

Figure 13 - Observation well 5, located to the left of horizontal well 1. The black line represents layer 1 (shallowest), the red line represents layer 2, and the blue line represents layer 3 (deepest). The plot also includes pressure buildup 40 days prior to hydraulic fracturing.

Long Term Pressure Response Trend 3:

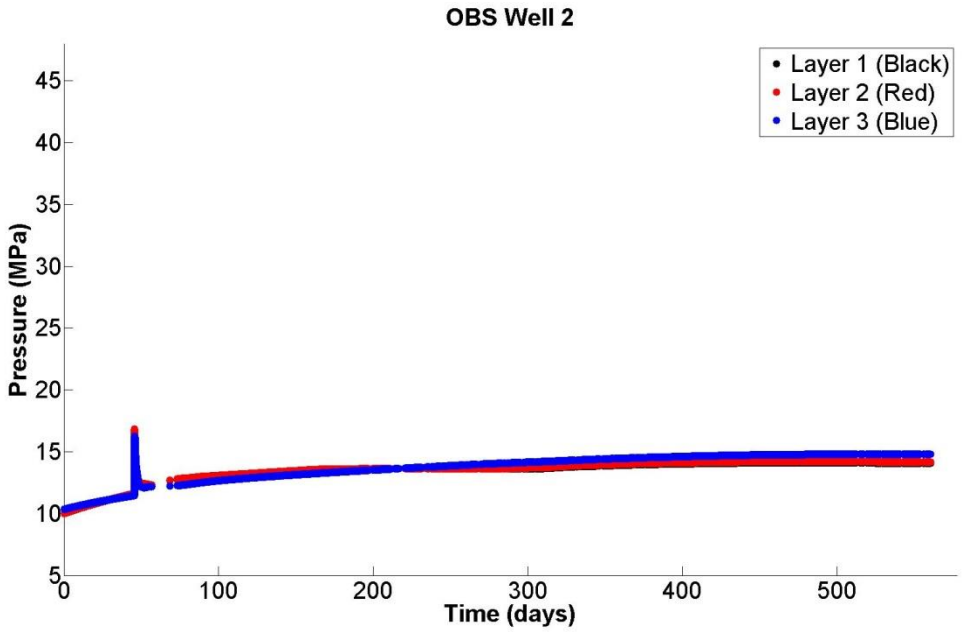

Figure 14 - Observation well 2, located to the left of horizontal well 1. The black line represents layer 1 (shallowest), the red line represents layer 2, and the blue line represents layer 3 (deepest). The plot also includes pressure buildup 40 days prior to hydraulic fracturing.

2.3 Discussion of short term pressure trends

During hydraulic fracturing, all of the vertical observation wells (except for one) recorded a rapid pressure increase. This suggests that the stimulated fracture network was both volumetric and complex. If planar fracture features were the predominant mechanism for stimulation, then some of the newly created fractures would likely have missed or not interacted with the observation wells. This was not observed. This result is somewhat tempered because the observation wells had previously been depleted.

Propagating hydraulic fractures should tend to propagate towards depleted regions, where stress has been reduced by the poroelastic response to pressure depletion. The data collected from the microseismic monitoring equipment also indicated that the fracture network was volumetric and complex.

Another interesting aspect of the data was that there was fairly sparse microseismicity at some of the vertical observation wells. This was despite the fact the pressure sensors at those wells recorded a large pressure increase. Figure 17 shows observation wells 2 and 5 had a limited number of microseismic events near them. However, they were still in the general vicinity of microseismicity, even though they were not in an especially active area. A potential explanation for the relatively limited seismicity in the vicinity of these wells could be the Kaiser effect, which is described in more detail in Section 4.8.

Another trend that was consistent throughout the data set, and unsurprising, was that the observation wells that were closer to the stimulated horizontal wells, tended to record larger pressure increases compared to the wells that were further away from the horizontal wells. Qualitatively, this observation makes sense because there should have been a lower pressure drop in the fracture (due to friction or fluid leak-off into the surrounding rock matrix) for the observation wells that were closer to the horizontal wells.

Interpretation of pressure trends at the vertical observation wells was complicated by the previous stimulation and depletion of the wells. Short term trend 1 clearly indicated that fluid from hydraulically fracturing (of the horizontal wells) came into

direct contact with the vertical observation wells through newly created hydraulic fractures. According to basic fracture mechanics, in order for a fracture to propagate through a formation, the fluid contained within the fracture must exceed the minimum principle stress (Paulding, 1967; Hubbert and Willis, 1972). When the pressure exceeds the minimum principal stress, the rock is placed in a state of tension which allows the fracture to propagate (Paulding, 1967; Hubbert and Willis, 1972). Because the pressure signal at wells of type 1 trend (very rapid pressure response, above the minimum principal stress) it would follow that this pressure trend was a direct result of newly created hydraulic fractures forming a direct connection to the vertical observation wells.

Interpretation of short term trend 2 was difficult, and there were two possible scenarios that could describe the pressure response at observation wells of type 2 trends. Type 2 trend was a rapid pressure increase, but below the minimum principal stress. If the vertical wells had not been previously stimulated, we could reasonable conclude that the pressure response at the vertical observation wells was caused by fluid flow through preexisting natural fractures only. Hydraulic fractures would have required a fluid pressure greater than the minimum principal stress. In contrast, fluid flow could occur through natural fractures at pressure less than the minimum principal stress. The natural fractures could be stimulated by shear.

However, because the vertical observation wells were previously stimulated, they were probably connected to highly conductive, preexisting pathways containing proppant. The highly conductive pathways (from the previous stimulation) could provide a direct connection to the vertical observation wells that remain conductive to fluid even

at pressure less than the minimum principal stress. The pathways created by the legacy hydraulic fractures could have artificially diverted stimulation fluid from their path of propagation. Because these legacy hydraulic fractures may have a non-negligible storativity, pressurization of these legacy fractures would not necessarily occur instantaneously because they require a significant volume of fluid in order to be pressurized. If pumping from hydraulic fracturing was stopped before the legacy network had a chance to be fully re-pressurized, the short term pressure signal of type 2 could occur.

The interpretation of short term trend 3 was that the previously created hydraulic fractures were only slightly connected to the vertical observation wells, and because of this, fluid was unable to flow at a high enough rate to induce a rapid pressure response. This could have occurred if the legacy hydraulic fractures were not fully propped or if proppant degradation occurred over time. This could also have occurred if the connection was only through weakly stimulated natural fractures.

Trend 4 represents a poroelastic pressure response at the vertical observation well. As noted previously, poroelastic responses in the formation were minimal due to the high fluid compressibility. Nevertheless, this is the one example in the data set that appears to be a poroelastic response. Observation well 6 was more than 500 ft. (152 m) away from horizontal well 1 and recorded a very slight pressure increase (<14 psi (0.096 MPa), Figure 10).

2.4 Vertical Connectivity between Formation Layers

A majority of the observation wells during stimulation recorded different pressure vs. time signals in the different formation layers. Observation well 9 (Figure 15) showed that the pressures sensors in the different layers had different signals during hydraulic fracturing. Layer 2 (blue line) had more kinks in the data than either layer 1 (black line) or layer 3 (red line). The maximum recorded pressure for layer 2 and layer 3 were approximately the same, but occurred at different times, and the maximum pressure recorded in layer 1 was about 2,000 psi less than the other two layers. The rate at which the pressure declined after the maximum recorded pressure occurred at different rates for the three layers.

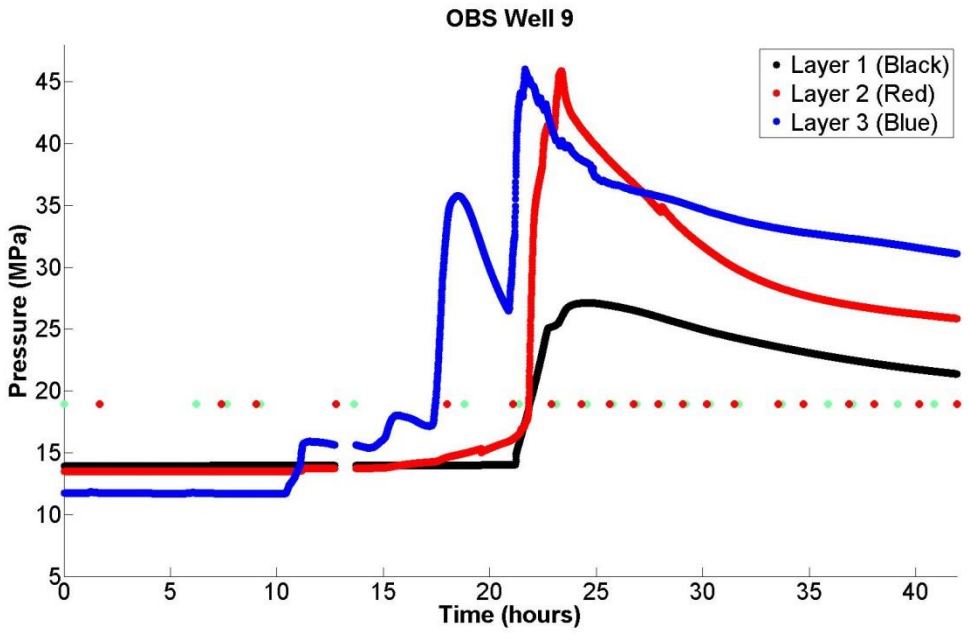

Figure 15 - Observation well 9, located to the right of horizontal well 4. Green dots represent the start of stimulation for a stage. Red dots represent when stimulation of a stage was completed. The black line represents layer 1 (shallowest), the red line represents layer 2, and the blue line represents layer 3 (deepest).

Observation well 4 (Figure 16) was the best example from the data in which the pressure vs. time trends for the different layers recorded similar signals, and the pressures declined at similar rates.

The different pressure signals within the formation layers suggest that vertical fracture growth during stimulation can occur at different times, different rates, or not at all in some layers. However, despite this trend, the long term pressure vs. time signals in general moved together, implying that the vertical fracture growth had less of a long term impact on depletion of the formation fluid (qualitatively).

Even though the data suggested different pressure signals within the different formation layers, the general observation that the pressure sensor located in the same formation layer the horizontal well was landed in, usually recorded the largest pressure response. This would imply the targeted layer was being stimulated.

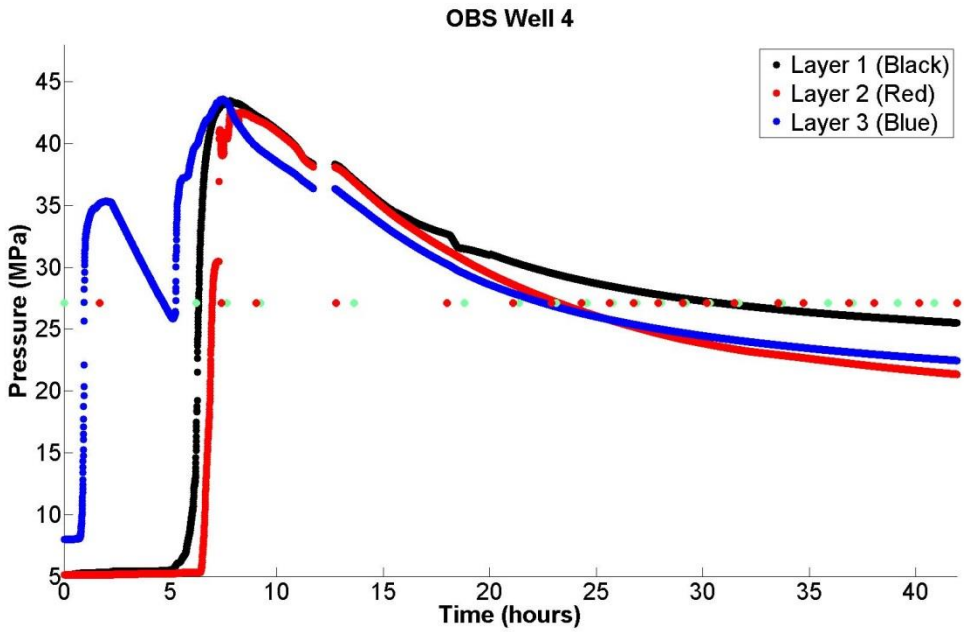

Figure 16 - Observation well 4, located to the left of horizontal well 4. Green dots represent the start of stimulation for a stage. Red dots represent when stimulation of a stage was completed. The black line represents layer 1 (shallowest), the red line represents layer 2, and the blue line represents layer 3 (deepest).

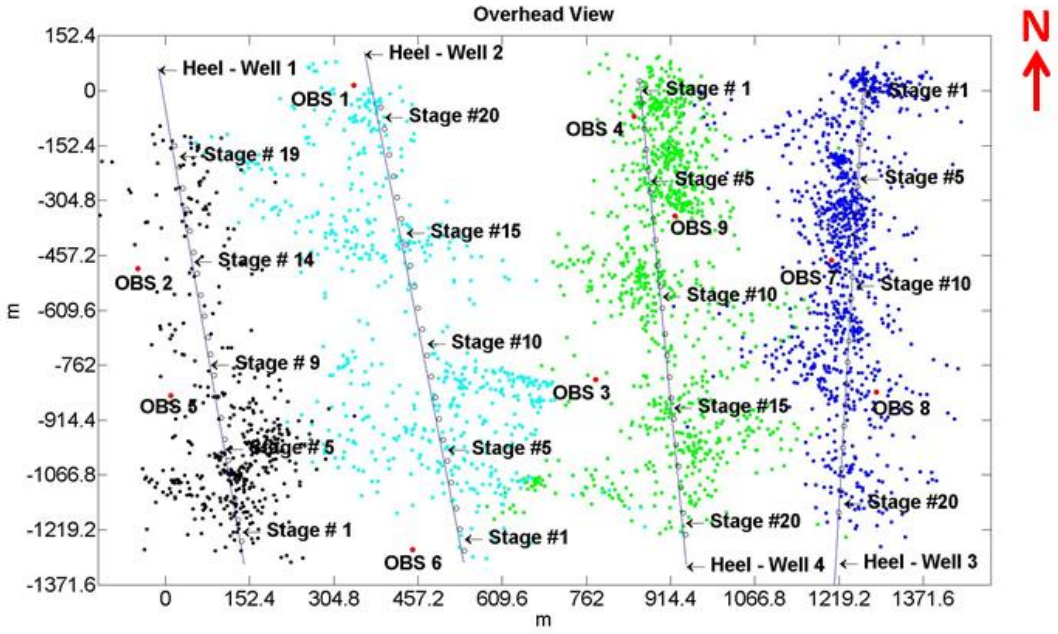

Figure 17 – Overhead view of the 4 horizontal wells. Also included on the plot are the microseismic events recorded during stimulation. The black colored microseismic events correspond to those that were recorded during stimulation of horizontal well 1. The cyan colored events correspond to those that were recorded during stimulation of horizontal well 2. The blue colored microseismic events correspond to those recorded during stimulation of horizontal well 3. The green colored microseismic events correspond to those recorded during stimulation of horizontal well 4.

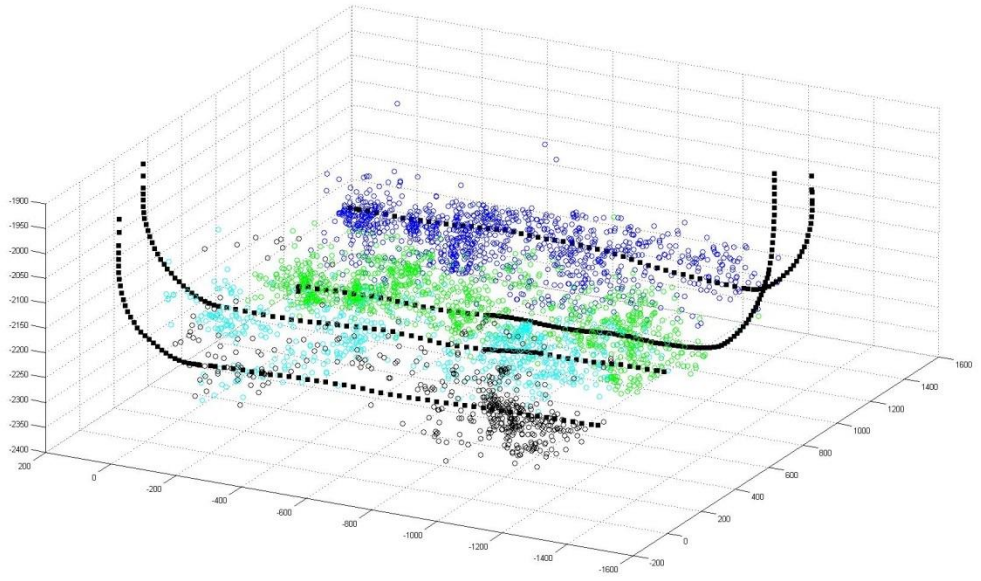

Figure 18 – 3 dimensional overhead view of the 4 horizontal wells that were hydraulically fractured. The same color scheme as Figure 17 was used in this plot. The black, solid square dots represent the wellbore of the horizontal wells. The vertical extent of the microseismic events was about 656 ft. (200 m).

Table 4 – Data in the table includes the number of microseismic events that were recorded during the stimulation of each of the horizontal wells. The average distance of microseismic events from the horizontal wells is also provided in the table.

Well #	# of MEQ events	Average distance from well (ft.)	Average distance from well (m)
1	445	179.1	54.6
2	593	319.6	97.4
3	1018	167.0	50.9
4	1044	225.4	68.7

2.4 Discussion of Long Term Pressure Trends

The most unusual trend from the long term pressure data was that some of the vertical observation wells showed a unique UP-DOWN-UP-DOWN pressure signal. This was an initial pressure increase, followed by a rapid pressure decrease, followed by another pressure increase, followed by a final pressure decrease (although a much more gradual decrease than the initial pressure decrease). In some of the wells, an UP-DOWN-UP trend was observed.

We believe that these observations can be explained by the previous stimulation and depletion of the vertical observation wells. During fracturing of the horizontal wells, newly created hydraulic fractures were able to interact with preexisting natural fractures (or legacy hydraulic fractures from the vertical wells) found within the formation. These interactions created a large, volumetric fracture network that allowed for stimulation fluid to flow and form a direct connection to the vertical observation well. Because of the

hydraulic connection, the pressure sensors recorded a large and rapid pressure increase at most of the vertical wells.

During and after hydraulic fracturing, injection fluid leaked off into the surrounding rock matrix. Because of the previous production of the vertical observation well, the rock matrix surrounding the vertical observation wells had a much lower reservoir pressure than the unproduced formation. Therefore, leakoff should have been especially rapid in the region around the observation wells. Fluid leakoff into the matrix explains why there was a very large and rapid pressure decrease after stimulation.

The second pressure increase, which occurred after stimulation but before production began, was probably the most interesting and anomalous aspect of the data set. We hypothesize that the second pressure increase was caused by flow of reservoir fluid from un-depleted formation towards the depleted region around the vertical wells. This region of depleted pressure was newly connected to the surrounding formation by the fractures created during stimulation of the horizontal wells. This could have allowed reservoir fluid from the un-depleted part of the formation to flow back towards the observation wells and re-pressurize them at a rate greater than normal reservoir build up.

Long term pressure data from observation well 5 (Figure 13) and observation well 8 (Figure 40) show that the rate at which the second pressure increase occurred was greater than the rate at which pressure buildup occurred while the observation wells were shut in. This could imply the second pressure increase was from un-depleted formation fluid being connected to the observation wells from newly created hydraulic fractures.

After this second pressure increase, there was a long term pressure decrease that was a result of production from the horizontal wells. This can be seen in the gradual decrease in pressure during the 18 months of recorded data.

It is important to highlight the difference between the pressure signal associated with fluid leakoff and the pressure signal associated with long term production. The pressure signal that results from fluid leakoff was rapid and occurred within hours, whereas the signal from long term production was more gradual. Using observation well 4 (Figure 16 – Short Term Pressure response and Figure 41 – Long Term Pressure response) as an example, fluid leakoff after stimulation was approximated to be 100 psi/hr (0.69 MPa/hr) (after peak pressure was recorded) and the rate at which pressure decreased from production of reservoir fluid was estimated to be 2 psi/day (0.014 MPa/day).

By comparing the wells that showed a long term pressure decline and the wells that did not, we were able to make qualitative observations about the relationship between fluid progression during hydraulic fracturing and depletion.

During hydraulic fracturing, fluid tended to extend further into the formation than the region that was depleted during production (also described by Barree et al., 2005; Cipolla et al., 2008; Manchanda et al., 2014). This could be observed from the three wells that were the furthest distance from the horizontal wells, observation wells 2, 3, and 6 (Figure 14, Figure 43 and Figure 19).

Observation wells 2 and 6 recorded a pressure increase during stimulation of horizontal well 1, indicating that they had been reached by injection fluid. Observation

well 3 did not record any data during stimulation, because the pressure sensors were off. Of the three wells, only observation well 6 showed a long term pressure decline, which implied the formation near observation well 6 was being depleted.

Observation well 6 was the closest to a horizontal well (~300 ft. (91.4 m) from well 2). Observation wells 2 and 3 were ~370 ft. (112.8 m) and ~435 ft. (132.6 m) away, respectively, from the nearest adjacent horizontal well.

Based on this qualitative analysis, it is reasonable to conclude that the stimulation fluid from hydraulic fracturing penetrated further into the formation than the region of depletion. We might conclude that the producing length of the hydraulic fracture did not extend much further than about 300 ft. from the horizontal wells. This is information is useful because future horizontal wells could be placed closer to one another (laterally) to improve recovery of formation fluid.

A potential explanation for why there was no reservoir fluid being depleted in the region near observation wells 2 and 3 is that proppant was not transported all the way to those wells.

Observation wells 2 and 6 had pressure response trends of type 2 and 3 during stimulation (a pressure increase that was below the minimum principal stress). There is no data available for observation well 3. The implication may be that proppant transport was severely limited (or non-existent) because the natural fractures were mechanically closed (net pressure below zero). Nevertheless, the stimulated fracture network was conductive enough for long term production of fluids found near observation well 6 (Figure 19) but not conductive enough deplete the formation near observation well 2

(Figure 14). Based on our initial hypothesis for the mechanism of stimulation, this suggests that in some instances natural fractures stimulated as a result of shear failure can contribute to production, but not necessarily.

After comparing the different pressure trends at the observation wells, it was determined that the hydraulic fracture half-lengths were on the order of 435 ft. (132.6 m) and perhaps even longer. The producing length of the hydraulic fractures tended to be shorter, and could be estimated to be at least 300 ft. (91.4 m), but no more than 370 ft. (112.8 m)

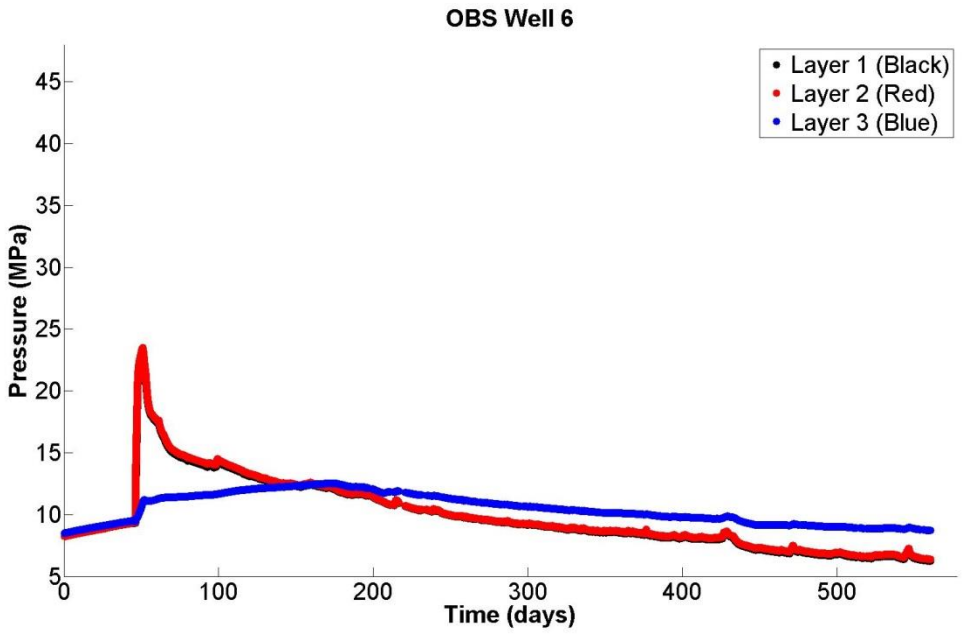

Figure 19 – Observation well 6, located to the left of horizontal well 2. This is a plot of the long term pressure response at the observation well. The black line represents the shallowest formation layer, the red line represents the middle layer, and the blue line represents the deepest formation layer. The plot also includes pressure buildup 40 days prior to hydraulic fracturing.

Chapter 3: *Modeling Approach*

Chapter 3 introduces the hydraulic fracture simulator that was used for the modeling aspect of this work. Chapter 3 also discusses the modeling approach that was used in order to match the simulation results to the trends that were observed in the field data set. Lastly, the chapter discusses some of the limitations of the simulator that was used.

3.1 Modeling Approach

The hydraulic fracture simulator used in this work was CFRAC, which stands for Complex Fracture ReseArch Code. The code was developed by McClure and Horne (2013). CFRAC is a discrete fracture-network simulator that couples fluid flow with the stresses induced by fracture deformation, both opening and sliding. A full description of CFRAC can be found in McClure and Horne (2013). Our simulations included a fully numerical treatment of fluid leak-off from the fractures and flow in the matrix.

Simulation parameters were varied in order to match the observed net pressure and the far field observation well pressures. Net pressure is defined as the pressure minus the formation minimum principal stress.

Cipolla et al. (2008) provide a general description of net pressure matching:

"Net pressure history matching is the activity of changing fracture model inputs and assumptions to calculate a model net pressure that matches the observed net pressure response. In most cases, the number of variables used to obtain a net pressure history match is limited to a handful of parameters. Note that these matching parameters are general and do not pertain to any specific model. A net pressure match can generally be obtained by matching both level and decline slope (during shut down periods) of net pressure using the following "level" and "slope" parameters."

One of the drawbacks with a net pressure history matching is that it can be very difficult to accurately estimate the bottom hole injection pressure, which is critical for performing a good analysis. Downie et al. (2015) stated that some of the challenges in calculating the bottom hole injection pressure are: that it is difficult to take into account (1) loss of pressure from pipe friction, (2) changes in slurry density, and (3) pressure drop across perforations in the casing (Downie et al., 2015).

Included in our data set were estimates of the bottom hole injection pressure. Pressure was measured at the surface, and then the service company calculated the bottomhole pressure. In addition to the pressure measurements at the well, we had pressure measurements at the observation wells.

Many of the simulation parameters were chosen based on the information provided by the operator. For example, diagnostic fracture injection tests (DFIT) had previously indicated the formation permeability was as high as 4 μd. The DFIT permeability was used because it produced simulation results that were in better agreement with the observation well data (see Section 4.2 Short Term Pressure Response Trend 1). Because net pressure history matching is nonunique different permeability values could be used to obtain the same simulations results.

The average injection rate during hydraulic fracturing was about 55 barrels per minute. The average time required to fracture one stage was roughly one hour. There were several instances when the time required for fracturing took significantly longer

than one hour. One example of this was during hydraulic fracturing of horizontal well 1, pumping of several stages was interrupted because of pump related issues.

The hydraulic fracturing fluid had an approximate viscosity of 25 centipoise. A limitation of our model was that we had to assume the fracturing fluid was single component, single phase with constant viscosity. The reservoir fluid was assumed to be the same as the injection fluid.

Some parameters from the data set were not provided because there is no simple method for quantifying them (e.g., vertical fracture growth). In order to come up with a reasonable value for vertical fracture growth, we referred to 3-dimensional microseismic images and the pressure vs. time data at the observation wells. After analyzing the data, we felt that 656 ft. (200 m) was a good starting point for our simulations; eventually we ran simulation where we varied fracture height from 246 ft. (75 m) to 656 ft. (200 m).

Wellbore imaging logs were not available, which meant there was no information available about the natural fractures in the formation. In sensitivity analysis, we found that the predicted net pressure was highly dependent on the natural fracture orientation. Some of the parameters that were available for us to change were: natural fracture density, natural fracture orientation, natural fracture length, natural fracture conductivity (or transmissivity), and fracture height (out of plane dimension).

As with any modeling, we faced the issue of accuracy vs. efficiency. For this work, we simplified the problem domain to include only one well, with one stage. Multiple wells with multiple stages are options that are available in CFRAC. However, the simulation time increases with the number of wells and stages. The simulations were

particularly computationally intensive because we chose to do a fully numerical treatment of leakoff and flow in the matrix, rather than a 1D leakoff approximation. Typical simulation time on an Intel i7 3.4 GHz, 32 GB RAM desktop PC was about 3 hours.

3.2 Model Limitations

There were several limitations to the simulator, and they are:

- CFRAC assumes the fracturing fluid (and reservoir fluid) is isothermal, slightly compressible, and single phase.
- CFRAC assumes the formation is homogenous. In addition, because the simulator that was used for this work was 2-dimensional, it was unable to take into account the different stresses of the different formation layers.
- The current version of CFRAC does not account for poroelastic stress perturbations that are created due to fluid flow in the matrix.
- CFRAC does not currently contain a proppant transport function.
- In CFRAC, potentially forming hydraulic fractures must be specified before the simulation is carried out. In addition, the potentially forming hydraulic fractures are assumed to be straight lines.

Chapter 4: *Simulation Results*

Chapter 4 introduces a simulation of a simple bi-wing fracture and explains why this fracture geometry could not match trends in the field data. Simulations with complex fracture networks were then used to obtain a baseline simulation. After the baseline simulation was established, the different short term and long term pressure trends were modeled. The results from these simulations are also discussed.

4.1 Baseline Simulation

The goal of our baseline simulation was to find a set of model parameters that would give us a net pressure that was close to the net pressure from the data set. In addition, we wanted to make sure the distance of fluid progression from the well was in general agreement with the field data (e.g., microseismic data and the pressure vs. time data at the vertical observation wells).

Our first simulation was of a bi-wing, planar fracture (with no preexisting natural fractures in the formation) that extended laterally away from the wellbore. The purpose of this simulation was to see if: (1) the results could produce similar far field observation well pressure as the data, (2) show that a bi-wing fracture geometry could not replicate the net injection pressure required for stimulation and, (3) show that a complex fracture network was the best solution for similar far field pressures as the observation wells.

Fluid was injected at a rate of 55 bbl/minute for 1 hour after which the well was then shut in. The simulation continued to run for an additional 110 hours (of simulation time) to allow for the fracture to continue growing after injection had stopped. The

average net pressure for the simulation was 58 psi (0.4 MPa) (the minimum principal stress was assumed 5,510 psi (38 MPa), based on the service company interpretation of the DFIT tests) and the hydraulic fracture half-length was 2,133 ft. (650 m), see Figure 20. In general, we were targeting a net pressure that was on the order of 1,595 psi (11 MPa) and fluid progression around 165-328 ft. (50-100 m). The target net pressure came from ISIPs and the minimum principal stress data was provided by the service company.

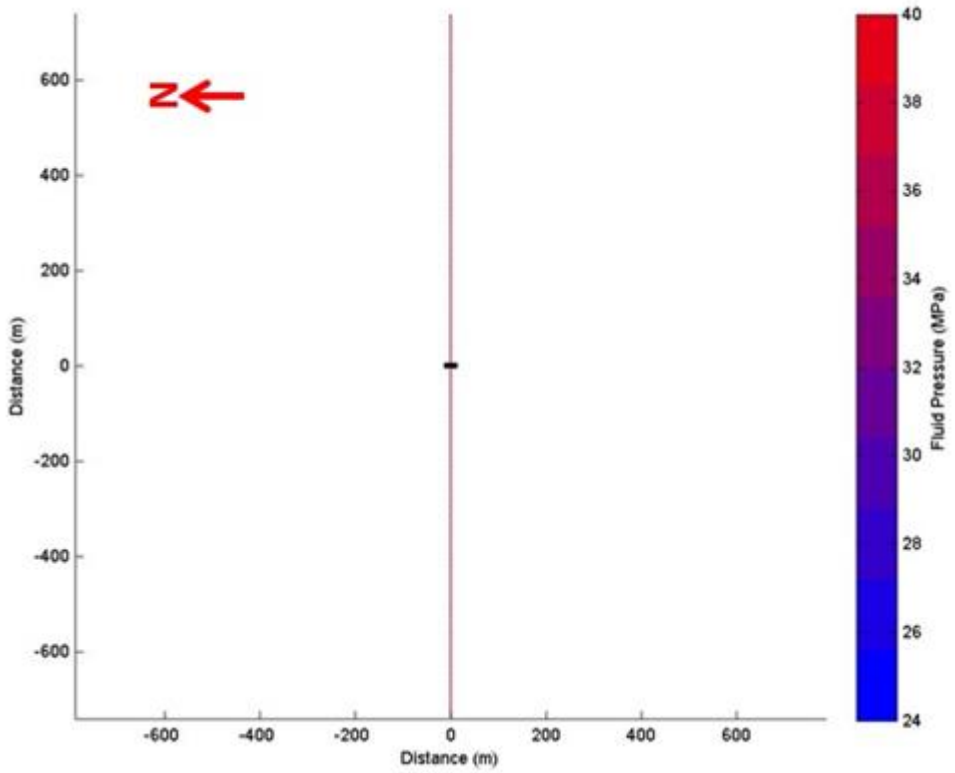

Figure 20 – Results from a bi-wing hydraulic fracture simulation. The black line in the middle of the figure is the wellbore. The red line extending up and down (y-direction) in the figure represents a newly created hydraulic fracture. The average net injection pressure for the simulation was about 0.4 MPa. The average net injection pressure from the field data set was about 11 MPa.

The simple bi-wing fracture simulation produced unrealistic results. The very long fracture and very low net pressure was consistent with typical simulation results from classical fracturing models (McClure et al., 2015). The biggest unknown in the data set was the lack of information about the preexisting natural fracture network. The next logical step was to establish a fracture network that provided a close match between the net injection pressure from the field data and simulation results. A trial and error approach was used until we obtained adequate results.

CFRAC generates preexisting natural fractures stochastically by using an external C++ code called input_gen.cpp. Input_gen also serves the purpose of discretizing the problem domain. This code was also developed by McClure and Horne (2013).

Input_gen requires the user to specify preexisting natural fracture properties such as the total number of natural fractures desired in the simulation, the minimum, the maximum, and the average length of the natural fractures. It also requires the user to specify if potentially forming hydraulic fractures are allowed to form (off the tips of the natural fractures). Additional parameters such as the minimum allowable angle of intersection between two natural fractures and the minimum distance between two adjacent natural fractures can also be specified. If these criteria are violated, the natural fractures that violate the constraints will not be included in the final fracture network. These properties can also be applied to potentially forming hydraulic fractures.

For our first attempt of simulations with natural fractures, we used a fracture network that was completely random in orientation. The purpose of this was to generate

data that would help us determine which natural fracture properties of the simulator had the biggest impact the results.

Fluid was injected into the wellbore for 1 hour, followed by a period of shut in. The simulation continued to run for nine hours (of simulation time) to allow for fluid through natural fractures. The average net pressure was about 145 psi (1 MPa). Figure 21 shows that fluid progressed about 656 ft. (200 m) in all directions. The results were unrealistic because in general fracture growth/fluid progression should predominately be in the direction perpendicular to the minimum principal stress. The simulation results show that there was limited growth of newly created hydraulic fractures. Most of the fluid flow was through natural fractures only.

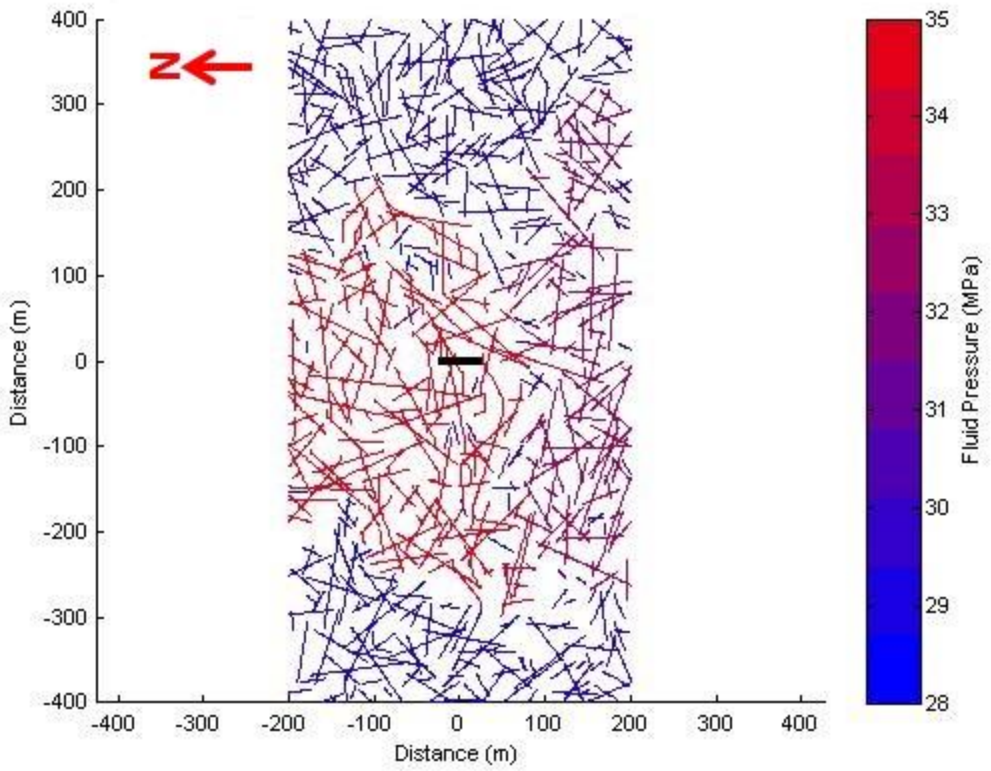

Figure 21 – Simulation results from a fracture network with completely random orientation. The red lines in the figure represent fractures that have been pressurized with fluid. The north/south growth of fluid progression from this simulation was on the order of 656 ft. (200 m). The east/west growth of fluid progression from this simulation was also about 656 ft. (200 m).

Next, we manually adjusted the orientation of the natural fracture network. This was accomplished by adjusting parameters used by input_gen. The expectation was that we could change the orientation of the natural fractures such that the net injection pressure would increase and the distance of fluid progression would decrease. This was done by altering the statistical distribution of the natural fractures that input_gen

generates. For these simulations, a wide range of preexisting natural fracture orientations were tried as well as different natural fracture densities.

Eventually, reasonable results were achieved with the fracture network shown in Figure 22. For this simulation, fluid was injected at a rate of 55 bbls/min for 1 hour, followed by shut in. The average net pressure was about 2,320 psi (16 MPa). We targeted a net pressure of 1,595 psi (11 MPa). This simulation net pressure was a big larger than observed, but at least qualitatively, it was of the same magnitude, unlike the initial set of simulations that were performed. There was also qualitative agreement between distance of fluid progression from the simulation results (164 ft. (50 m) – 328 ft. (100 m)) and the data set.

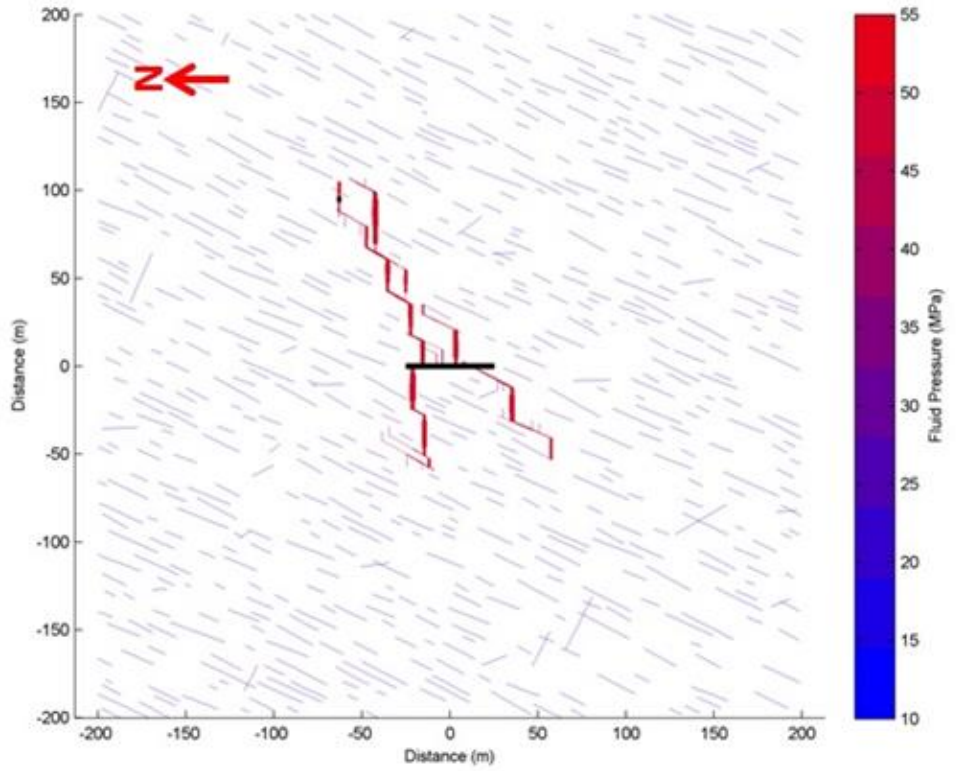

Figure 22 – Results from our calibrated baseline simulation. Fluid from hydraulic fracturing extended about 164 ft. (50 m) – 328 ft. (100 m) into the formation, which was in agreement with the data set. The average net pressure for this simulation was about 2,320 psi (16 MPa).

After establishing the baseline simulation, we attempted to model all the short term pressure response trends (except the poroelastic pressure response) and the long term pressure trends from the data set. For the pressure response simulations, we needed to take into account the effect of the previous stimulation and depletion of the vertical observation wells. This was accomplished by creating a legacy hydraulic fracture that intersected the vertical observation well. For this hydraulic fracture, we assumed that it had a half-length of about 62.5 ft. (19 m). Also, because the legacy hydraulic fracture

probably contained proppant, we specified that it should have a higher conductivity than the other surrounding fractures.

For the long term and short term pressure trend simulations, there were two wellbores in the problem domain (Figure 23): (1) a vertical well represented by a point intersecting a legacy hydraulic fracture, and (2) a horizontal well represented by a line that was 195 ft. (59.4 m) in length, the equivalent of one stage.

We produced the vertical well for approximately 10 years (using the production pressure and rates that were provided to us by the operator), followed by a period of shut in of six months to one year. After shut-in, the horizontal well was then hydraulically fractured for 1 hour, and then shut-in.

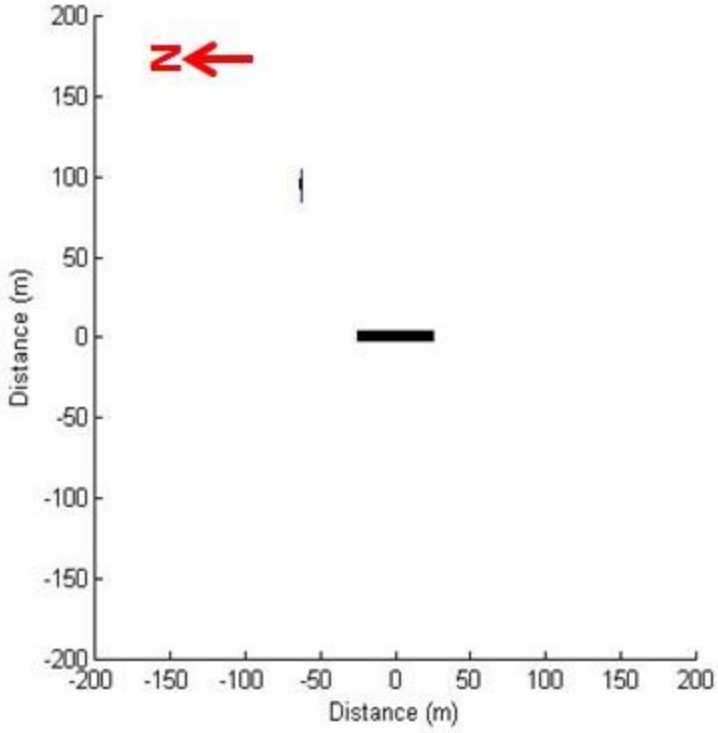

Figure 23 – Image of the horizontal well bore (black line) at the center of the figure and the vertical observation well in the upper left side of the figure. The vertical well is represented by a point. The blue line that intersects the vertical wellbore is the legacy hydraulic fracture that was created 10 years earlier.

4.2 Short Term Pressure Response Trend 1: Simulations 1 and 2

Short term trend 1 was a rapid pressure increase that was above the formation minimum principal stress and then a rapid pressure decrease. This must have been due to direct hydraulic connection to the injection well.

The field data we attempted to match was of observation well 5 (Figure 7). Figure 26 shows the pressure vs. time results from simulation 1. The simulation results show there was a very large and rapid pressure increase above the minimum principal stress, but not a sufficiently rapid pressure decline after stimulation stopped. The field data had a maximum observation well pressure of 6,500 psi (44.8 MPa) compared to a maximum pressure of 6,862 psi (47.3 MPa) from the simulation results.

There was general agreement in the maximum pressure and the distance of fluid progression between the simulation results and field data. However, there was a major discrepancy in the rate at which pressure declined after fluid injection stopped. In the field data, pressure declined almost immediately after hydraulic fracturing, and in the simulation there was almost no pressure decline after injection stopped.

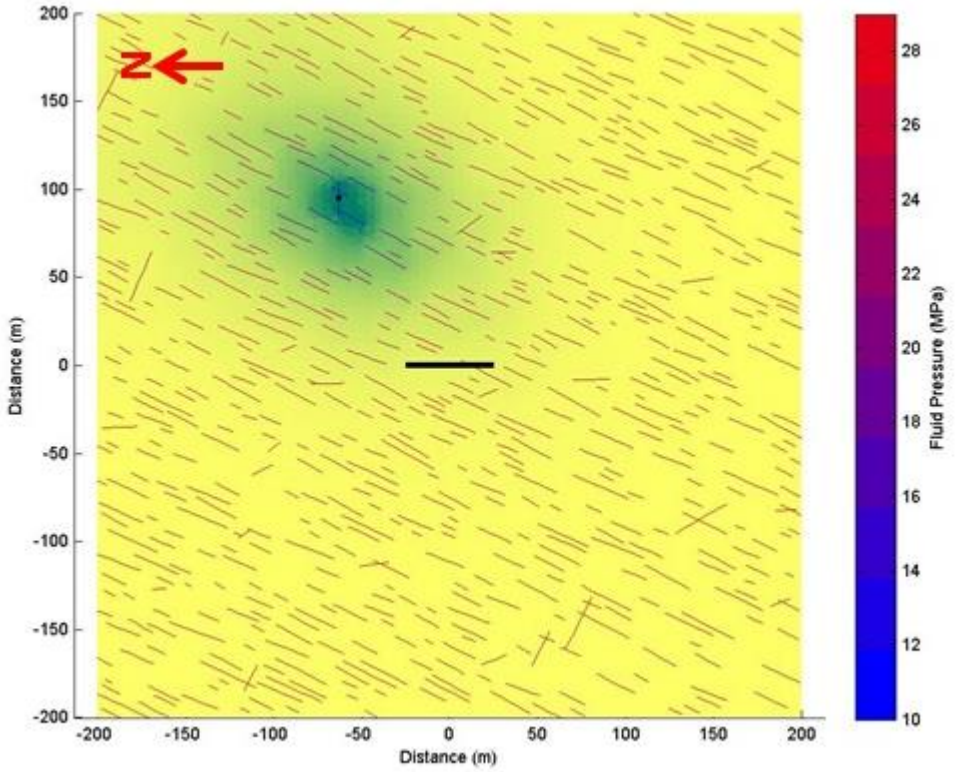

Figure 24 – Simulation results after the formation was produced for a period of ten years. The green halo represents the portion of the formation that has been depleted.

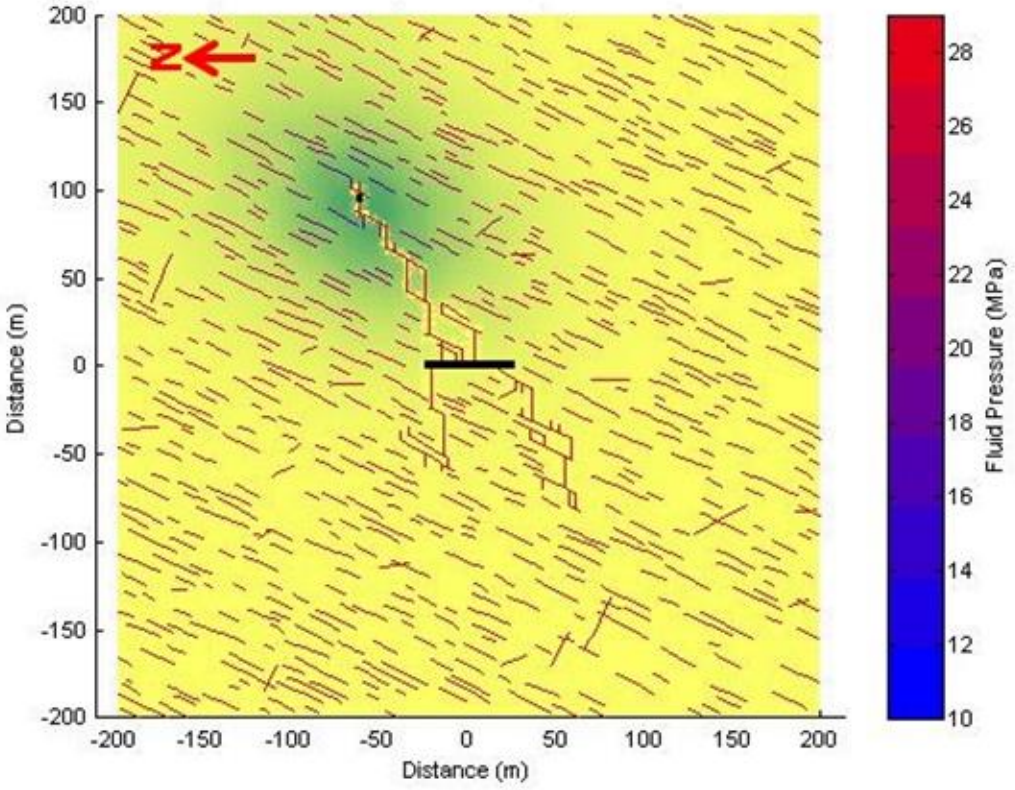

Figure 25 – Simulation results after hydraulically fracturing the horizontal well. The red lines represent fractures with high fluid pressure. The newly created fractures from stimulation intersect the vertical observation well.

In order to better match the simulation results to the field data, we had to flow back the horizontal well immediately after injection. Simulation 2 used the same parameters as simulation 1, with the only difference being that simulation 2 had flow back after hydraulic fracturing. Including flow back was the only way to get the pressure to drop at a rate that was similar to what was observed in the field data.

This was not the ideal solution to the problem. In hydraulic fracturing operations, fluid is flowed back only after all stages in a well are stimulated. Figure 7 shows that the pressure from the field data decreased decrease immediately after the completion of the

stage and not after all the stages in the well were fractured. This suggests that the pressure decline was from fluid leak-off and not from flow back of the horizontal well.

We feel a more accurate solution would to better incorporate the complex fluid interactions between stimulation fluid and the rock matrix. Accurately modeling fluid leak-off into the surrounding rock matrix is difficult in any simulator, but it is particularly difficult in CFRAC because of the single phase, single component fluid assumption we used. This assumption over simplifies the complex interactions that occur between the two fluids. For example, Dehghanpour et al (2012) show that spontaneous imbibition and "the organic material and reactive clay minerals can influence the liquid flow in the small pores of shale." These interactions can be significant and need to be considered in order to accurately model fluid leak-off.

Another issue is that the model assumed that the viscosity of the fluid leaking off was the same as the viscosity of the fluid in the fracture, 25 cp. But the large polymer molecules in the fracturing fluid would almost certainly be too large to enter into the pore space of the formation. The viscosity of the polymer-free filtrate entering the formation would be similar to the viscosity of water, which would be on the order of tenths of a cp at the reservoir temperature. Lower viscosity during leakoff would increase leakoff volume.

To summarize, we suspect that our inability to properly model the rapid pressure depletion after shut-in was caused by multiphase/multicomponent flow effects that could be not described by CFRAC.

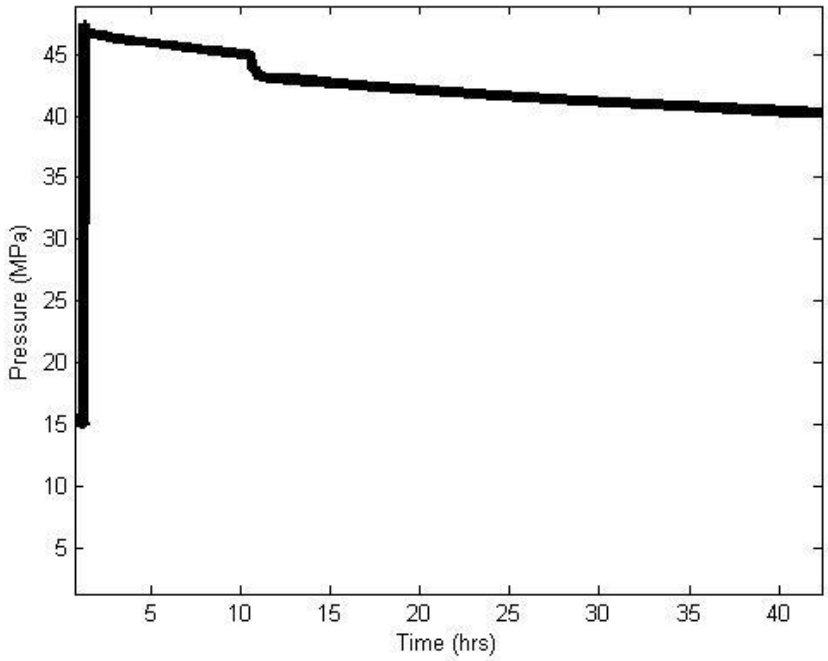

Figure 26 – Pressure vs. time results from the vertical observation well in Simulation 1. The results from this simulation do not include flow back of the horizontal well after stimulation. The maximum pressure achieved from the simulation qualitatively matches the maximum pressure from the field data (47 MPa vs. 44.5 MPa). The discrepancy between the two is the rate at which pressure decreases after hydraulic fracturing.

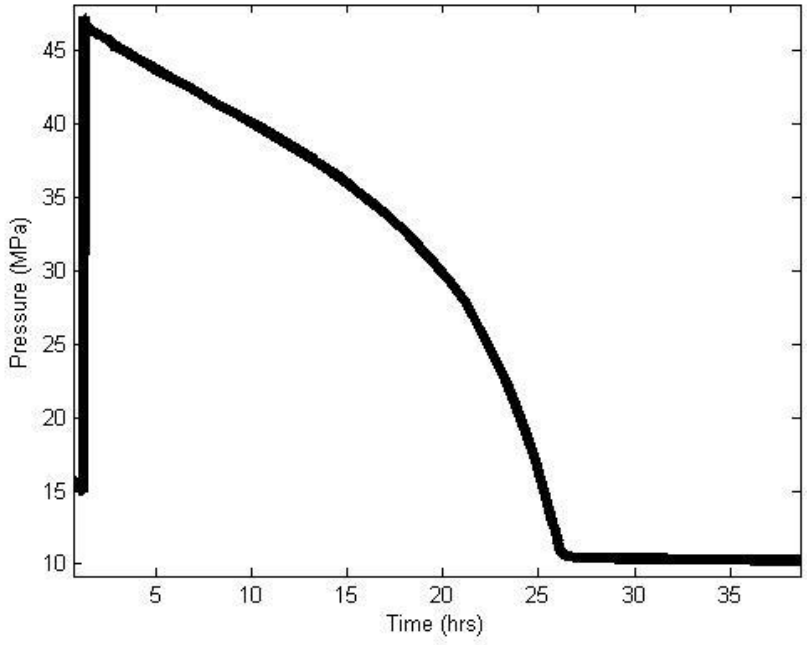

Figure 27 – Pressure vs. time results from the vertical observation well in Simulation 2. The results from this simulation include flow back of fracture fluid after stimulation. The maximum pressure achieved is the same as Simulation 1. This simulation captures the pressure decline more accurately than simulation 1.

4.3 Short Term Pressure Response Trend 2: Simulation 3

Trend 2 was a rapid pressure increase, but below the minimum principal stress. After the pressure increase, there was either: (1) a rapid pressure decrease or (2) a gradual pressure decrease. Based on our hypothesis, the difference between trend 1 and 2 was the type of connection between the horizontal well and vertical observation well. For type 2 trends, the connection to the vertical well was predominately from preexisting natural fractures or from the legacy hydraulic fracture intersecting natural fractures in the formation.

The field data we were trying to match was observation well 7 (Figure 8). The same fracture network used in simulations 1 and 2 was also used for simulation 3. Conceptually, once the stimulation fluid reached the vertical observation well, we wanted the fluid pressure within the natural fractures to be below the minimum principal stress so the fractures would be mechanically closed and not open. This was achieved by adjusting the conductivity of the natural fractures. The results from the simulation are shown in Figure 28.

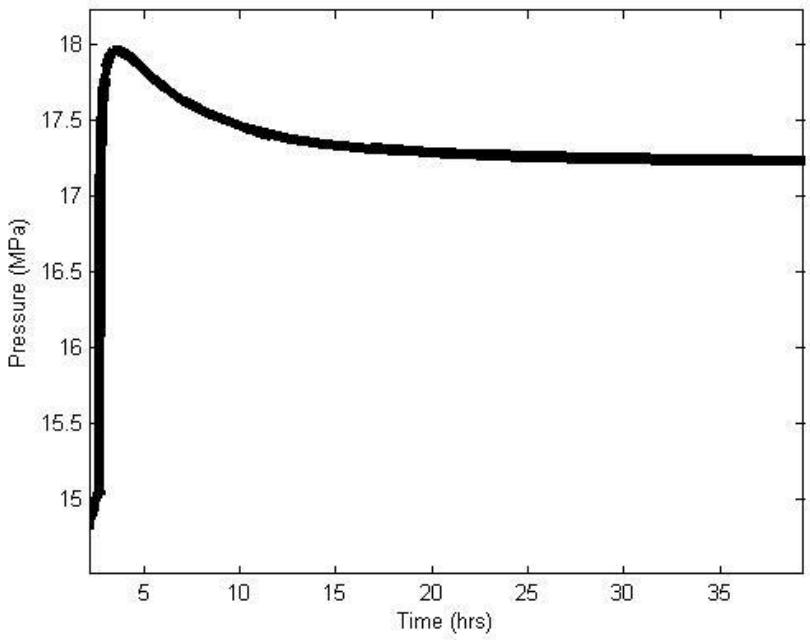

Figure 28 – Pressure vs. time plot from simulation 3. A maximum pressure of 18 MPa was recorded from the stimulation compared to a maximum pressure of 22 MPa.

The results from simulation 3 had a maximum observations well pressure of 2,610 psi (18 MPa), comparted to the field data which had a maximum pressure of about 3,190 psi (22 MPa). Simulation 3 did not include flow back after the horizontal well was hydraulically fractured. We were able to get a good qualitative match between the pressure at the observation well and the simulation results. We attempted the simulation with flow back, but it did not alter the simulation results.

4.4 Short Term Pressure Response Trend 3: Simulation 4

Trend 3 represents a gradual pressure increase throughout the entire fracture treatment with the pressure at the observation well was always below the minimum principal stress. Our hypothesis for this trend was that the observation well was located outside a region of stimulated fractures and a pressure wave of fracturing fluid was able to leak-off from the fractures towards the observation well. The low pressure around the observation well (from the previous production) provided a pressure gradient that allowed for fluid to migrate. The result of this was a gradual pressure increase during stimulation.

The field data we attempted to match was of observation well 6 (Figure 9). Similar to simulation 3, we wanted a low natural fracture conductivity so that stimulation fluid would not be allowed to form a direct connection to the vertical observation well. We wanted there to be two different regions in the model (Figure 29): (1) a region containing a conductive fracture network that was connected to the horizontal wellbore,

and (2) a region containing the vertical observation well that was isolated from the conductive fracture network.

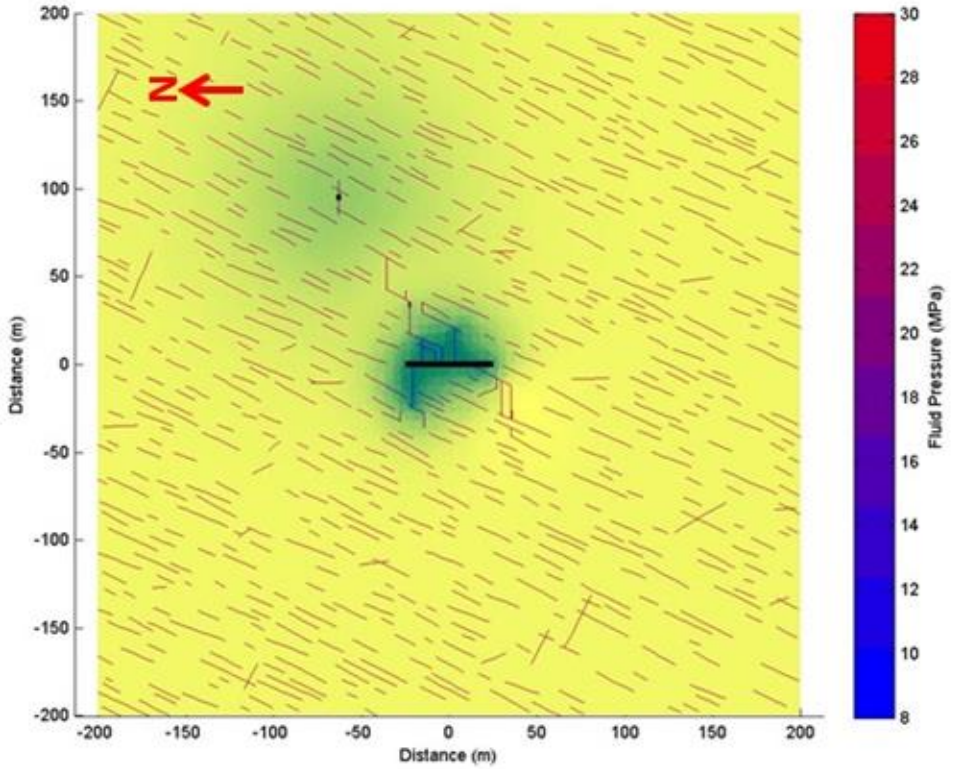

Figure 29 – Final image from simulation 5. In this image, the horizontal wellbore is in a highly conductive region of natural fractures. The vertical observation well is disconnected from this region. The pressure response at the vertical observation well is a byproduct of stimulation fluid leaking off into the matrix and migrating towards the well.

We were unsuccessful in matching the simulation results to the field data. The problem we faced was the network connection to the observation well was either hydraulically connected so that the pressure increase was too rapid and too large or the

observation well was too far away from the network so that there was no continuous pressure increase throughout stimulation.

4.5 Long Term Pressure Response Trend 1: Simulation 5

Long term pressure trend 1 was an UP-DOWN pressure response. The hypothesis for this trend was that the initial pressure increase was a result of newly created hydraulic fractures forming a direct connection to the vertical observation well. The subsequent pressure decrease was from the formation being depleted as a result of production from the horizontal well.

The pressure vs. time data from observation well 9 (Figure 12) was the field data we were trying to match. In order model this trend; we used the same simulation settings as simulation 2 (from short term trend 1 simulations). There were several minor differences between the two simulations. These differences were the rate and duration of flow back. The results from this simulation are shown in Figure 30.

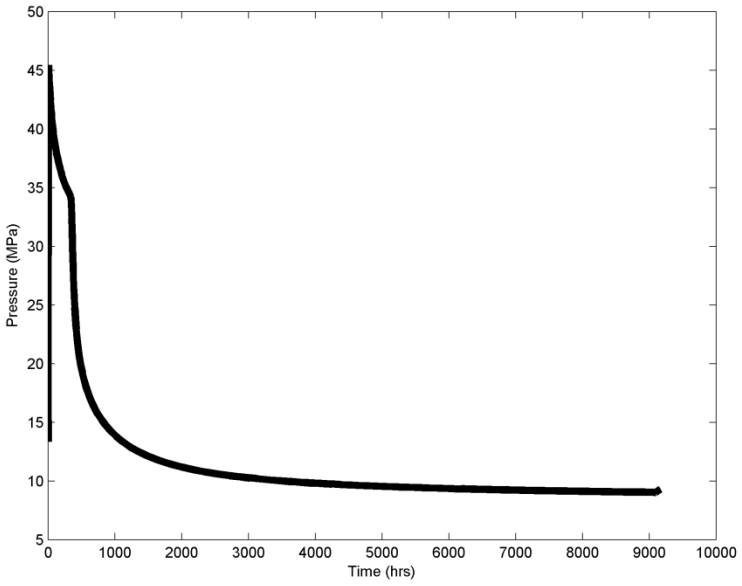

Figure 30- Pressure vs. time plot of result from simulation 5. This represents trend 1 from the long term pressure response data. This is an up-down trend.

4.6 Long Term Pressure Response Trend 2: Simulation 6

This model was attempting to match the long term pressure trend of observation well 5 (Figure 13). The pressure vs. time response was an UP-DOWN-UP-DOWN pressure signal. The hypothesis for this trend was that the initial pressure increase was from stimulation fluid forming a direct connection to the vertical observation well during hydraulic fracturing. The pressure decrease that followed was a result of fluid leaking off into the surrounding rock matrix. The second pressure increase was from the formation fluid migrating towards the low pressure zone near the vertical observation well (which was from the previous production of the vertical wells). The last pressure decrease was

from the fluid around the observation well being depleted as a result the horizontal well being produced.

For this simulation, the only way to get the UP-DOWN-UP-DOWN pressure trend was if we produced the horizontal well immediately after stimulation. If this was not done, we would not have been able to get a sufficiently rapid pressure decrease. As discussed above, we believe the difficulty in matching the data purely with leakoff was because the simulator did not include multiphase flow effects. After producing the horizontal for a short period, the well was then shut in for four weeks. This shut in period allowed for fluid to migrate back towards the vertical observation well and allowed us to get the second pressure increase. After the shut in period, the horizontal well was then produced at rate and pressure comparable to the production rates that were provided to us. The horizontal well was then produced for a total of 18 months.

Again, the simulation results (Figure 32) were in qualitative agreement with the field data. A maximum pressure of 8,265 psi (57 MPa) at the observation well was recorded. This was higher than the 6,453 psi (44.5 MPa) that was recorded from the data set. Despite this difference, the general trend from this simulation results were similar to the pressure vs. time data from the data set.

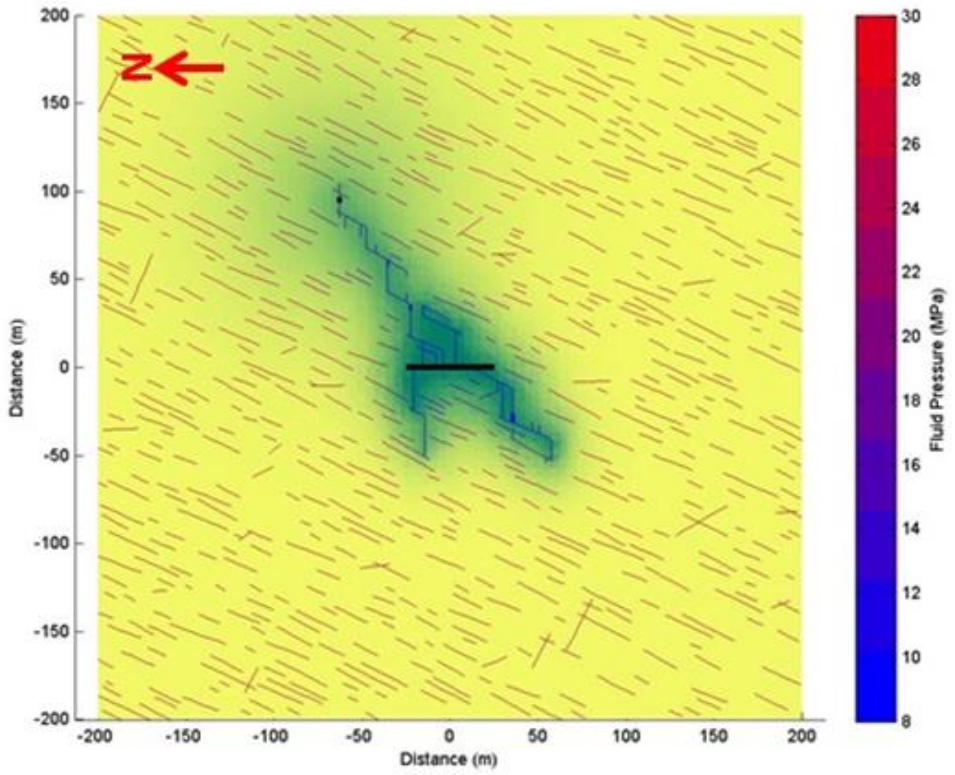

Figure 31 – Results from simulation 1. The blue halos in the plot represent depleted formation. The black line in the center of the figure represents the horizontal wellbore. Fluid progression was in the range of 22.9 – 30.5 ft. (75 – 100 m).

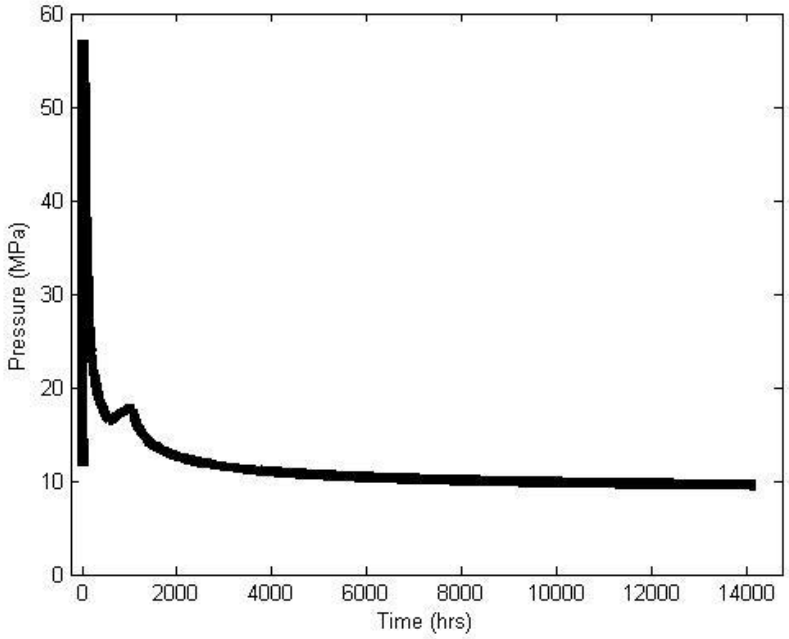

Figure 32 – Results from simulation 6. This simulation was attempting to match the UP-DOWN-UP-DOWN pressure trend that was recorded at observation well 5.

4.7 Long Term Pressure Trend 3: Simulation 7

The field data that we were trying to match was from the long term pressure vs. time data of observation well 2 (Figure 13). This trend was represented by an UP-DOWN-UP pressure signal.

The hypothesis for this was that there was an initial pressure increase below the minimum principal stress that was a result of hydraulic fracturing. The pressure decrease was from fluid leak-off into the surrounding rock matrix. The second pressure increase was from reservoir fluid migrating back towards the vertical observation well. The

explanation for the lack of pressure decline was that there was very little or no proppant transport through the natural fractures.

The results from this simulation are shown in Figure 14. There was qualitative agreement between the simulation results and field data. However, the second pressure increase (from fluid migration) was larger in the simulation results compared to the field data.

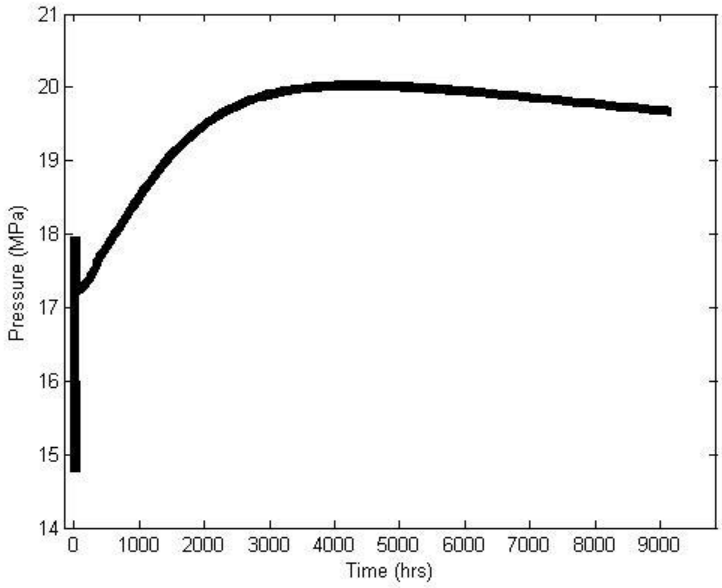

Figure 33 – Results from simulation 7. This simulation was attempting to match the long term pressure trend 3. The field data observation well we were trying to match was observation well 2.

4.8 Simulation of the Kaiser Effect

The theory to explain the Kaiser effect was first developed for homogenous materials, such as metal alloys, and gives an explanation for what happens when a

material is subjected to “cyclic loading”. These principals have also been extended to rocks and porous media (Holcomb, 1993).

As related to hydraulic fracturing, the Kaiser effect is a phenomena in which fluid (from stimulation) can invade areas of a formation without being detected by microseismic monitoring equipment (even if the equipment is within the appropriate range for investigation and capable of detecting microseismic events). A microseismic event is a small shear slip on a preexisting fracture that releases energy and is recorded by either surface equipment or downhole geophone arrays. This shear slip, which is a byproduct of an increase in fluid pressure from the stimulation, creates a zone of permanently relaxed stress. If the fluid pressure is increased again (cyclic loading), microseismic events may not be recorded. This can occur if an adjacent stage has been previously stimulated and the new fractures connect to the previously stimulated fractures. If the fluid pressure that invades the previously stimulated fractures is greater than the maximum pressure achieved during the previous stimulation, then there will be microseismic events. But if the pressure remains below the previous maximum pressure, then microseismic events will not be recorded (Baisch et al., 2006; Baisch et al., 2009).

This data set contains an example of the Kaiser effect. During stimulation of horizontal well 4, the pressure sensor found within layer 3 of observation well 8, recorded a pressure increase of approximately 1,800 psi (12.4 MPa) (Figure 34). Observation well 8, was located more than 1,000 ft. (304.8 m) away from horizontal well 4. No microseismic events were detected in the vicinity of observation well 8 during stimulation of horizontal well 4 (Figure 35).

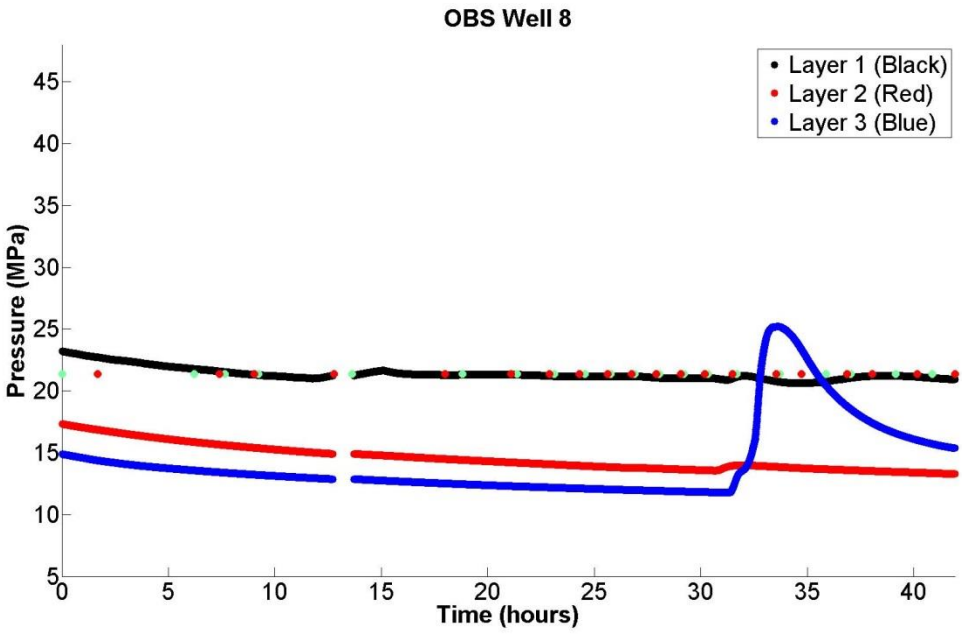

Figure 34 – Pressure vs. time data recorded at observation well 8 during stimulation of horiztonal well 4. This pressure increase was from stimulation fluid from well 4. Fluid was able to interact with the fracture network created from stimulation of well 3. The pressure increase was below the formation minimum principal stress of 5,510 psi (38 MPa). Observation well 8 was located more than 1,000 ft. (304.8 m) away from horizontal well 4.

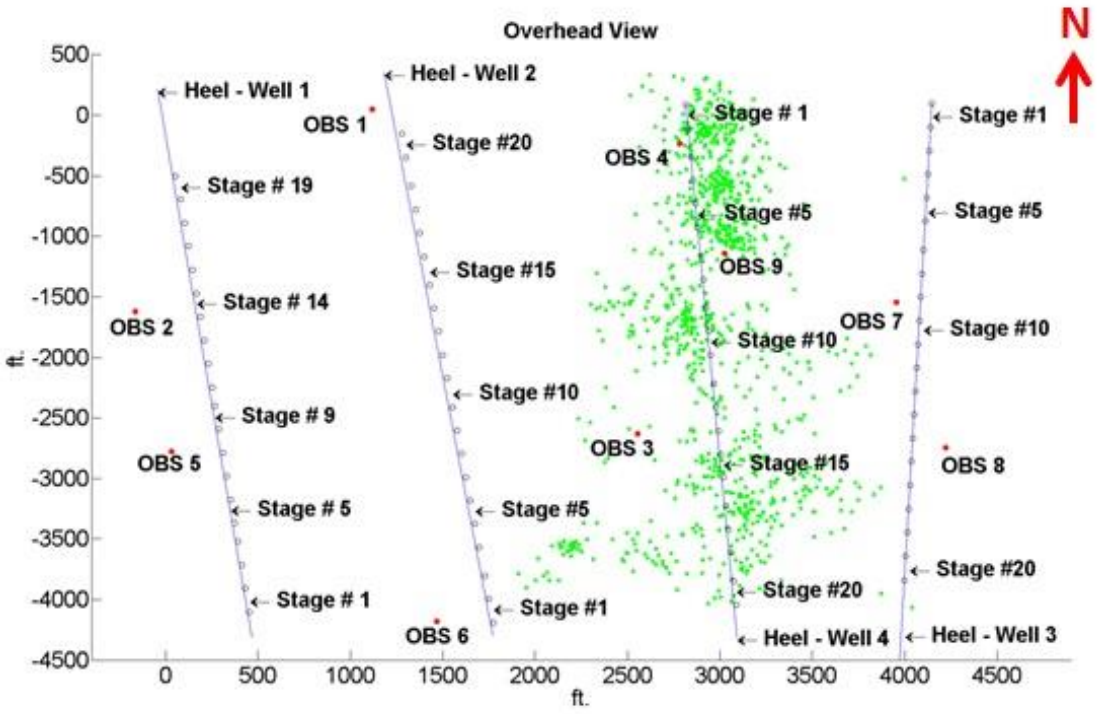

Figure 35 – Microseismic events recorded during stimulation of horizontal well 4. The purpose of this figure is to illustrate that there were no associated microseismic events near observation well 8 despite the fact observation well 8 recorded a pressure increase during stimulation of well 4.

The general explanation could be that the hydraulic fractures created from stimulation of horizontal well 4 were both volumetric and complex, and connected to the fracture network that was created during stimulation of horizontal well 3 (horizontal well 3 was stimulated prior to horizontal well 4). As fluid injected into well 4 drained into the fractures created around well 3, the pressure increased but remained below the maximum pressure reached during the initial formation of the fractures around well 3. As a result, no microseismic events were recorded near observation well 8, despite the fact there was

a relatively large pressure increased recorded by the pressure sensors. The maximum pressure that was recorded at observation well 8 was 3,600 psi (24.8 MPa), which was well below the minimum principal stress of 5,510 psi (38 MPa).

In order to create a simulation that captured this phenomenon, we needed to have two horizontal wells in the problem domain. The fracture network that was created from hydraulically fracturing each of the wells needed to extend far enough into the formation so they intersected one another. We also needed the observation well to be within the pathway of one of these newly created hydraulic fracture networks.

We wanted the observation well to record a pressure increase above the minimum principal stress during the stimulation of the first horizontal well and then record another pressure increase below the minimum principal stress during stimulation of the second horizontal well.

The microseismic events from the simulation are shown in Figure 36 and the pressure vs. time of the observation well (from the simulation) is shown in Figure 37. Figure 36 shows two different microseismic clouds that were created during hydraulic fracturing. The red microseismic events were created during stimulation of the first well (bottom of the figure). The blue microseismic events were created during stimulation of the second well (top well of the figure). Similar to what we observed in the field data; there were no recorded microseismic events near the observation well (black dot) during stimulation of the second horizontal well. However, there was a rapid pressure increase recorded at the observation well during stimulation of the second horizontal well (Figure 37).

The synthetic microseismic events were created by tracking the displacement of each element in the problem domain. Microseismic events were generated only if the displacement of an element went above a specified threshold value. If the displacement was above the specified threshold, the location of the event was recorded. In order to prevent the microseismic events from being created only along the linear fracture pathways, normally distributed location error was included so that a cloud of microseismic events were created.

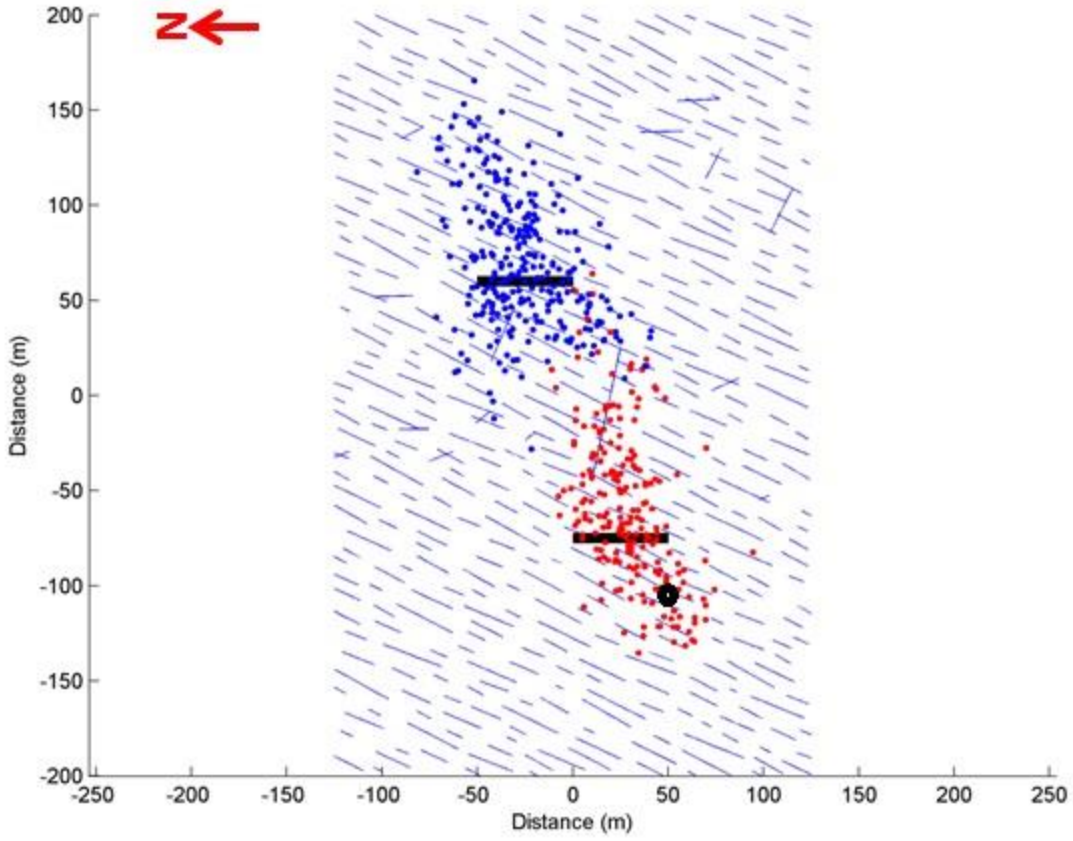

Figure 36 – Kaiser Effect simulation results from CFRAC. The black dot in the figure represents a vertical observation well. The bottom horizontal well in the figure was stimulated first. The red dots in the figure represent microseismic events that were created from hydraulic fracturing. The top horizontal well in the figure was stimulated second. The blue dots in the figure represent the microseismic events that were created from stimulation of the second well. There are no blue microseismic events anywhere near the red cloud of microseismic events, despite the fact that there was fluid progression in the fracture network. This shows that there was no microseismic response near the observation well despite the increase in pressure.

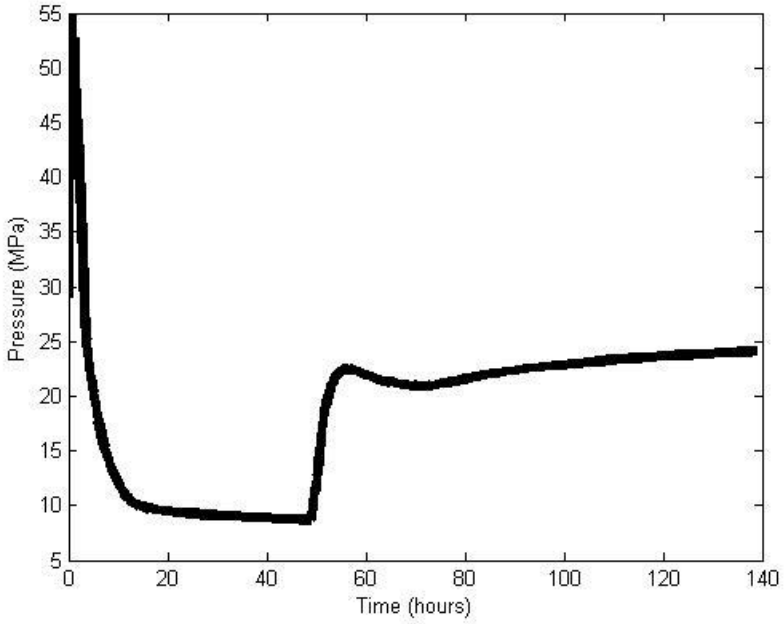

Figure 37 –Pressure vs. time results from the observation well in the Kaiser Effect simulation. The initial pressure increase is from stimulation fluid coming into direct contact with the vertical observation well in the problem domain. The pressure decrease is from producing back the horizontal well. The second pressure increase (around 50 hours) is from stimulation fluid from horizontal well 2 coming into contact with the vertical observation well.

4.9 Modeling Challenges

The biggest challenge we faced while modeling was accurately representing the rapid pressure decrease at the observation well after hydraulic fracturing. The field data showed that immediately after stimulation (within a matter of minutes to hours) the pressure began to decline rapidly. However, in our simulation results, the pressure would persist and not decline at a rate that matched what was observed from the data. The only

method available in CFRAC to match the field data was to flow back fluid immediately after stimulation (e.g., turn the well on for production). While this provided a nice qualitative match to trends in the field data, it does not accurately represent the actual physical phenomena that took place.

The most likely explanation for not being able to match the rapid pressure decrease after stimulation was that our model assumed the injection fluid was the same as the reservoir fluid and was single phase, single component. However, in reality, the fracturing fluid was a viscous linear gel and the reservoir fluid was a volatile, low viscosity oil. CFRAC models leakoff by using the 1D diffusion equation adapted from the work of Vinsome and Westerveld (1980) and requires the fluid to be single phase, with constant fluid properties (such as viscosity and compressibility).

The importance of using the appropriate fluid parameters can be conceptually illustrated by using the equation for leakoff in the reservoir zone from Economides and Nolte (2000). Fluid leakoff velocity is calculated as:

$$u_L = \frac{C_c}{\sqrt{t}}$$

Where Cc is the compressibility control leakoff coefficient and t is time. The compressibility control leakoff coefficient is calculated with the following equation:

$$C_c = \sqrt{\frac{k_r c_t \phi}{\pi \mu_r}} \Delta p_c$$

Where kr is the permeability of the reservoir rock, μr is the reservoir fluid viscosity, ct is the total fluid compressibility, ϕ is the formation porosity, and Δpc is pressure drop from the filtrate/reservoir and the far field reservoir.

This equation shows that if the total compressibility were increased and the reservoir fluid viscosity were decreased then the overall the compressibility leakoff control coefficient would increase. This would increase the overall fluid leakoff velocity and ultimately increase the total volume of fluid leakoff.

There can also be other complex fluid interactions that would cause fluid leakoff to occur more rapidly in reality when compared to the results from the simulations. One of these interactions could be fluid loss from spontaneous imbibition. The impact of fluid loss from spontaneous imbibition in shale formations can be significant (Dehghanpour et al. (2012); Markhanov et al. 2014) .We were also unable to take into account the interaction of fracturing fluids with clays that are typically found in shale formations (Dehghanpour et al. 2012; Markhanov et al. 2014).

Another explanation for why CFRAC could not accurately model fluid loss, but less significant, is that the resolution of preexisting fractures in CFRAC is unable to take into account micro-fractures that occur in real formations. The natural fractures created by CFRAC are on the order of 10s of meters in length which are much larger than micro-fractures in a formation (cm or smaller). These micro-fractures could accommodate volumes of fluid that potentially significant and not negligible.

One idea for a model improvement would be to take into account the multiphase interactions that occur with real fluids. This would require making significant

adjustments to CFRAC. Another option, would be to implement a matrix permeability function that would allow for greater rates of fluid leak-off as injection pressure is increased. With this function, fluid would be allowed to leak-off into the matrix at a higher rate while there is a high pressure within a fracture.

Another challenge was that some of our net pressures from simulation results were higher than what was in the field data set. For some of the simulations, they were modestly higher (15 MPa vs. 11 MPa from the data set). Despite this, we were successful in illustrating that a complex fracture network was necessary to get a net pressure that was in general agreement with the data. A simple bi-wing fracture produced unrealistic net pressure results. With further adjustment, we could have created a base case with net pressure equal to 11 MPa, but the base case was judged to be close enough to the simulation data.

Overall, despite some of the limitations, we think we were successful in matching (qualitatively) the simulation results to the field data. The vertical observation wells provided priceless data on the flow of fluid in the reservoir. Yet there exists only a few papers in the literature that discuss the use of offset wells to monitor lateral fluid progression or pressure at a discrete points within a formation (Dohmen et al., 2014; Downie et al., 2015).

Chapter 5: *Summary and Conclusions*

5.1 Summary

In this work I interpreted a field dataset that contained vertical observation wells surrounding four hydraulically fractured horizontal wells. The vertical observation wells provided pressure measurements over time at a variety of distances from the hydraulically fractured horizontal wells. This dataset is quite unique because far-field measurements of pressure during hydraulic fracturing are rarely available.

We categorized and analyzed the pressure trends at the observation wells and developed hypotheses to describe each of those trends. Modeling was performed with a hydraulic fracturing simulator in order to qualitatively match the simulation results of individual stages with the field data. Modeling of individual stages was done in order to allow for a large number simulations to be performed in a reasonable amount of time. In addition, the lack of heterogeneity included in the 2-dimensional hydraulic fracture simulator would most likely not change the simulation results when comparing the stimulation of an entire well vs. one stage.

5.2 Conclusions

The main results from this thesis are:

- The fracture network created during stimulation was both volumetric and complex. This was determined based on (1) microseismic data, (2) pressure vs. time data at the observation wells, and (3) results from our modeling. The modeling results show the net pressure from a simple bi-wing fracture is much lower than the net pressure that was required for fracturing in the data set. Creating a network of preexisting natural fractures was the only method available that produced simulation results with a high net pressure.

- The data set contained a clear example of the Kaiser effect. The Kaiser effect is a phenomenon in which fluid invades a previously stimulated region of a formation without generating microseismicity. Microseismicity does not occur due to the stress relaxation caused by the previous stimulation. Observation well 8 was located over 1,000 ft. away from horizontal well 4, but close to horizontal well 3. During stimulation of horizontal well 4 (performed after horizontal well 3), observation well 8 recorded a large pressure increase, but there were no microseismic events recorded near the well. This demonstrates that fluid injected at horizontal well 4 aseismically repressurized of a large region of the stimulated network surrounding horizontal well 3.
- The observation well data suggested the length of fluid progression (the hydraulic fracture half-length) was longer than the producing length of the hydraulic fracture (the effective hydraulic fracture half-length). This conclusion was based on long term pressure data at three observation wells. This observation has been described frequently in the literature (Barree et al., 2005; Cipolla et al., 2008; Manchanda et al., 2014). We examined wells that were 300 ft., 370 ft., and 435 ft. away from the nearest respective horizontal well. All three of these wells recorded a strong pressure increase during hydraulic fracturing, indicating a hydraulic connection to the observation well. However, only one of the wells (the one that was 300 ft. away) recorded a long term pressure decrease. This suggests that even though fluid reached the other two wells, the regions surrounding these wells was not depleted during long-term production.

5.3 Recommendations

The results suggest there may be opportunities for improvement in future hydraulic fracturing procedure.

- Some of fluid pumped during the stimulation of horizontal well 4 flowed into the fracture network surrounding well 3. This was aseismic due to the Kaiser effect and probably did not contribute to further stimulation surrounding well 3. However, the fluid probably leaked off into the surrounding formation and was not recovered during flowback. Therefore, this was an inefficient use of water. Care should be taken to avoid repressurizing the stimulated fracture network around neighboring wells during stimulation. This may be much more common than commonly recognized because the process is aseismic.
- The region of reservoir filled with injection fluid was larger than the region that was depleted during production. This was probably because injection fluid propagated ahead of the proppant and the unpropped fractures did not retain sufficient conductivity during depletion. This also represents an inefficient use of water. In addition, the pressure measurements suggest that there are gaps between the horizontal wells where fluid is not being efficiently drained. The measurements suggest that fluid was drained within about 300 feet of the horizontal wells, but the well spacing was commonly 750-1050 feet.
- It may be worth experimenting with well spacing closer to 600 feet than the 750-1000 feet used in the four wells in the dataset. However, this could exacerbate the problem of fluid leaking into the stimulated region of adjacent wells.

- Another solution could be to experiment with using a more viscous frac fluid with better proppant transport capability. A more viscous fluid would probably generate less complexity, but complexity is only valuable if the fractures remain conductive. The results suggest that in this formation, the unpropped fractures did not fully retain conductivity during depletion, suggesting that proppant placement should be emphasized over the generation of network complexity.

Appendix

The plots in the appendix include pressure vs. time data for all other observation wells that were included in the data set.

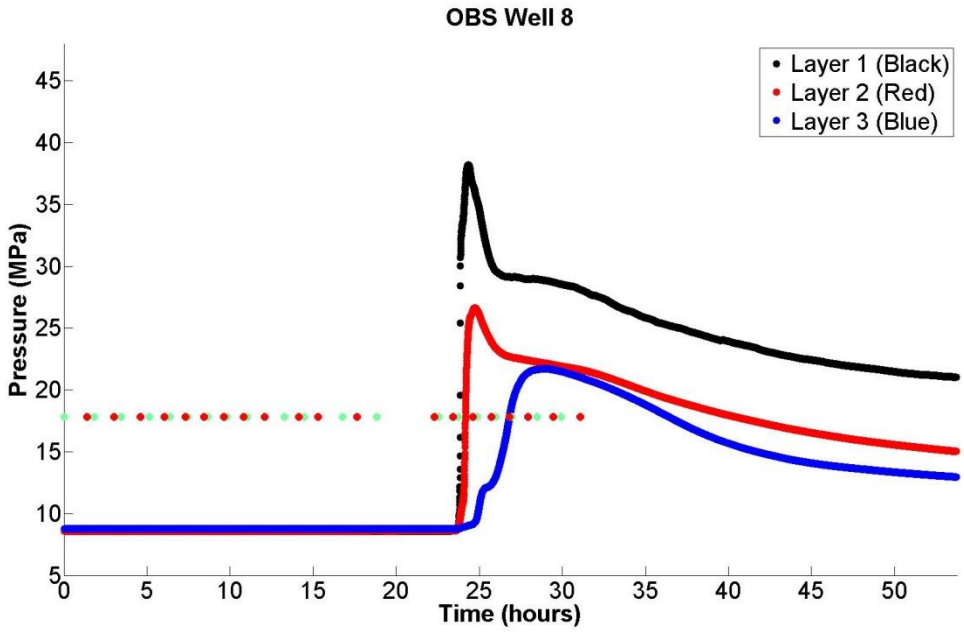

Figure 38 - Observation well 8, located to the right of horizontal well 3. Green dots represent the start of stimulation for a stage. Red dots represent when stimulation of a stage was completed. The black line represents layer 1 (shallowest), the red line represents layer 2, and the blue line represents layer 3 (deepest).

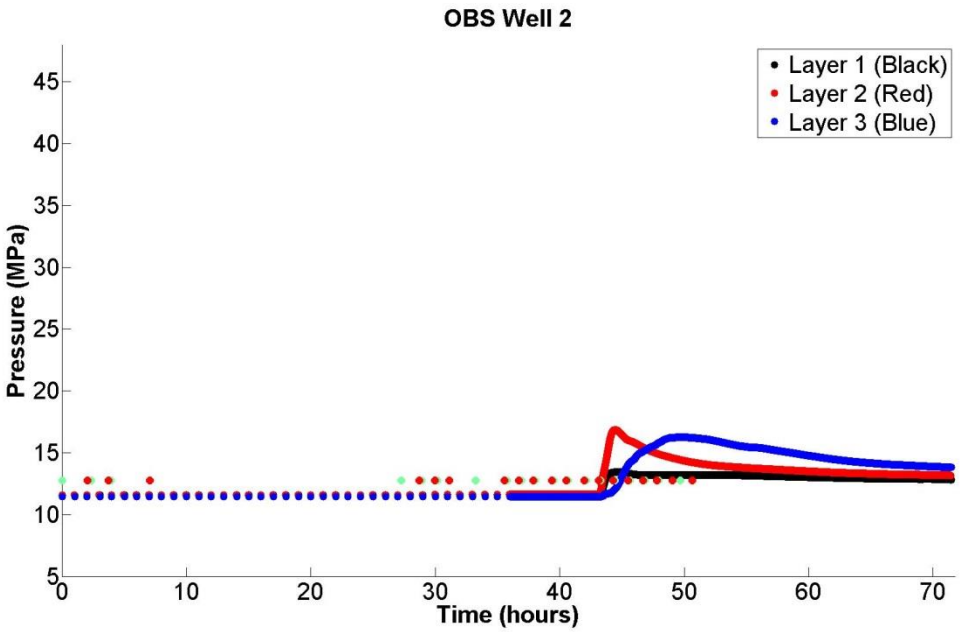

Figure 39- Observation well 2, located to the left of horizontal well 1. Green dots represent the start of stimulation for a stage. Red dots represent when stimulation of a stage was completed. The black line represents layer 1 (shallowest), the red line represents layer 2, and the blue line represents layer 3 (deepest).

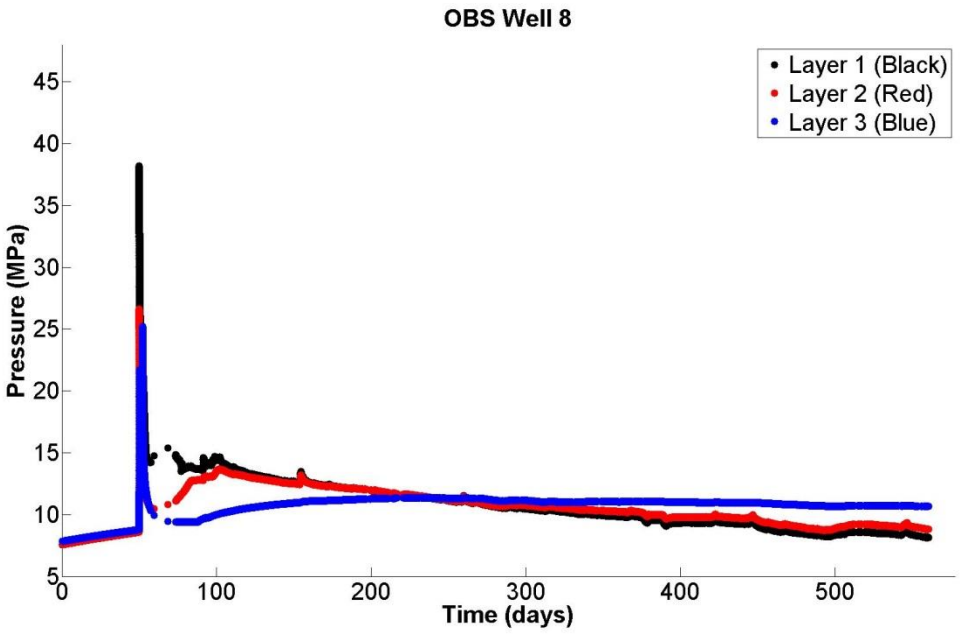

Figure 40 – Observation well 8, located to the right of horizontal well 3. This is a plot of the long term pressure response at the observation well. The black line represents the shallowest formation layer, the red line represents the middle layer, and the blue line represents the deepest formation layer.

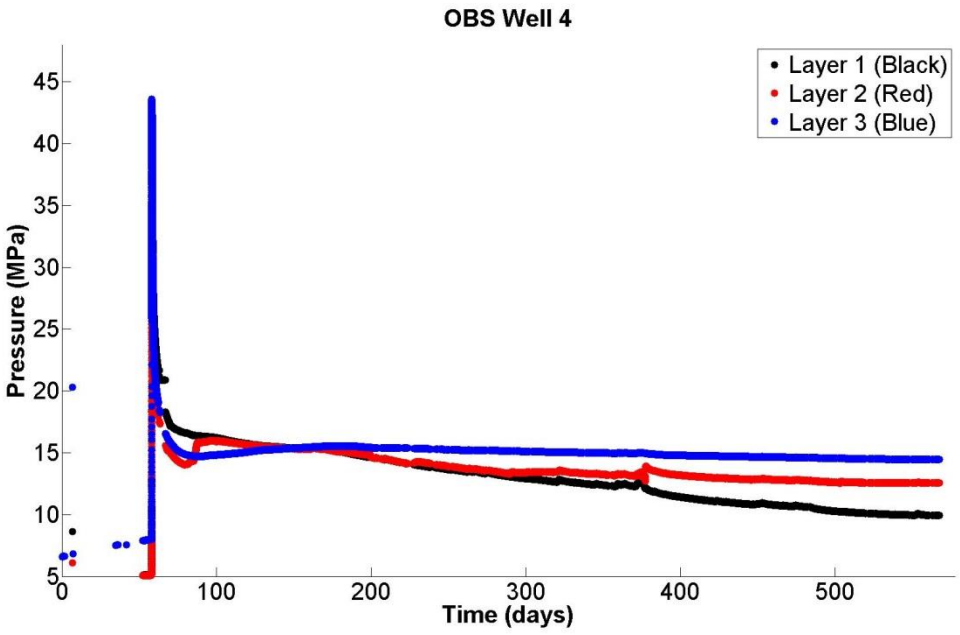

Figure 41 – Observation well 4, located to the left of horizontal well 4. This is a plot of the long term pressure response at the observation well. The black line represents the shallowest formation layer, the red line represents the middle layer, and the blue line represents the deepest formation layer.

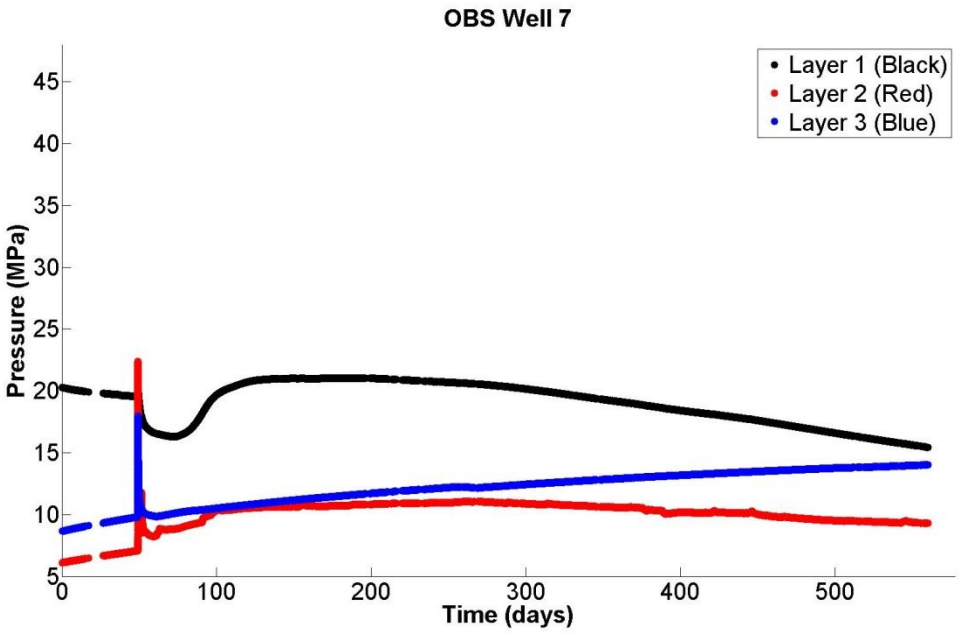

Figure 42 – Observation well 7, located to the left of horizontal well 3. This is a plot of the long term pressure response at the observation well. The black line represents the shallowest formation layer, the red line represents the middle layer, and the blue line represents the deepest formation layer.

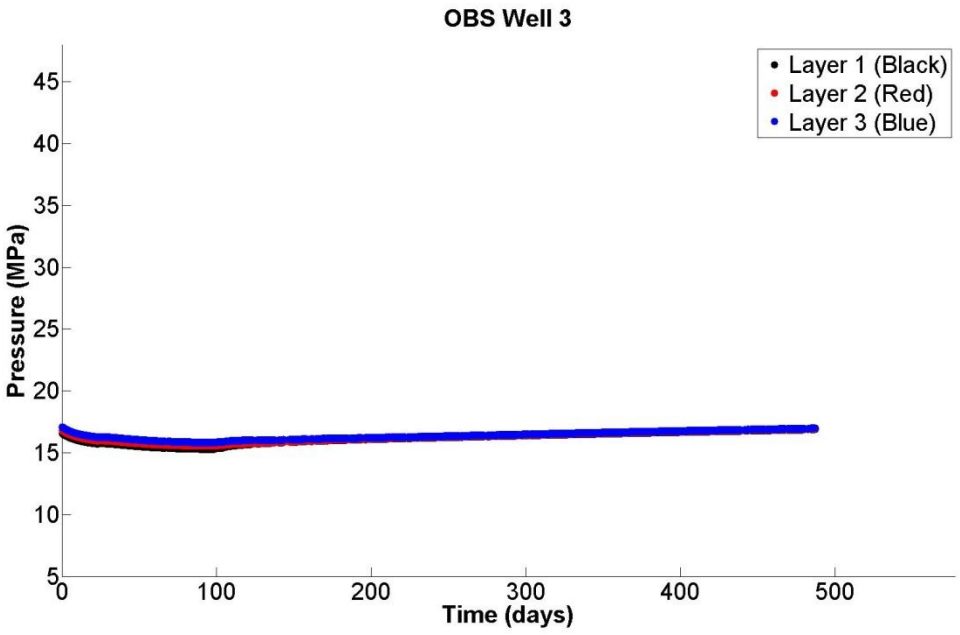

Figure 43 – Observation well 3, located to the left of horizontal well 4. Note, this well did not record pressure vs. time data during hydraulic fracturing of horizontal well 4. This is a plot of the long term pressure response at the observation well. The black line represents the shallowest formation layer, the red line represents the middle layer, and the blue line represents the deepest formation layer.

Table 5 –Simulation parameters

h (formation height)	*75-100m*	*μ_f (coefficient of friction)*	*0.6*
G (shear modulus)	*15 GPa*	*$\sigma_{n,Eref}$*	*50-90 MPa*
υ_p (Poisson's ratio)	*0.25*	*$\sigma_{n,eref}$*	*10-85 MPa*
S_0	*0.5 MPa*	*φ_{Edil}*	*0-2.5 degrees*
e_0	*0.00003-0.003 m*	*φ_{edil}*	*0-2.5 degrees*
E_0	*0.00005-0.02 m*	*E_0*	*0.00005-0.02 m*
P_{init} (initial fluid pressure)	*29 MPa*	*K_{Icrit}*	*2.5 $MPa\sqrt{m}$*
σ_{xx} (remote x-direction stress)	*38 MPa*	*Injection rate*	*146 kg/s*
σ_{yy} (remote xy-direction shear stress)	*56 MPa*	*μ (fluid viscosity)*	*24.7 cp*

References

Arguijo, A. L., Morford, L. S., Baihly, J., & Aviles, I. (2012, January 1). Streamlined Completions Process: An Eagle Ford Shale Case History. Society of Petroleum Engineers. doi:10.2118/162658-MS

Aviles, I., Dardis, M., & Marya, M. (2013, November 1). Degradable Frac Ball Holds Solution to Persistent Problem in Fracturing. Society of Petroleum Engineers. doi:10.2118/1113-0032-JPT

Baisch, S., Weidler, R., Vörös, R., & Jung, R. (2006). A conceptual model for post-injection seismicity at Soultz-sous-Forêts. GRC Transactions, 30, 601-605.

Baisch, S., Vörös, R., Weidler, R., & Wyborn, D. (2009). Investigation of fault mechanisms during geothermal reservoir stimulation experiments in the Cooper Basin, Australia. Bulletin of the Seismological Society of America, 99(1), 148-158.

Barree, R. D., Cox, S. A., Gilbert, J. V., & Dobson, M. L. (2005, November 1). Closing the Gap: Fracture Half Length from Design, Buildup, and Production Analysis. Society of Petroleum Engineers. doi:10.2118/84491-PA

Browning, J., Ikonnikova, S., Gülen, G., & Tinker, S. (2013, July 1). Barnett Shale Production Outlook. Society of Petroleum Engineers. doi:10.2118/165585-PA

Bybee, K. (2009, March 1). Resolving Created, Propped, and Effective Hydraulic-Fracture Length. Society of Petroleum Engineers. doi:10.2118/0309-0058-JPT

Cherian, B. V., Fields, K. W., Crissman, S. C., Itibrout, T., & Yates, M. E. (2009, January 1). Maximizing Effective Fracture Half-Length to Influence Well Spacing. Society of Petroleum Engineers. doi:10.2118/122514-MS

Cipolla, C. L., Warpinski, N. R., & Mayerhofer, M. J. (2008, January 1). Hydraulic Fracture Complexity: Diagnosis, Remediation, And Exploitation. Society of Petroleum Engineers. doi:10.2118/115771-MS

Cipolla, C. L., Weng, X., Mack, M. G., Ganguly, U., Gu, H., Kresse, O., & Cohen, C. E. (2011, January 1). Integrating Microseismic Mapping and Complex Fracture Modeling to Characterize Hydraulic Fracture Complexity. Society of Petroleum Engineers. doi:10.2118/140185-MS

Dahi Taleghani, A., & Olson, J. E. (2014, February 1). How Natural Fractures Could Affect Hydraulic-Fracture Geometry. Society of Petroleum Engineers. doi:10.2118/167608-PA

Damjanac, B., I. Gil, M. Pierce, and M. Sanchez (2010), A new approach to hydraulic fracturing modeling in naturally fractured reservoirs, ARMA 10-400, paper presented at the 44th U.S. Rock Mechanics Symposium and 5th U.S.-Canada Rock Mechanics Symposium, Salt Lake City, Utah.

Dehghanpour, H., Zubair, H. A., Chhabra, A., & Ullah, A. (2012). Liquid intake of organic shales. Energy & Fuels, 26(9), 5750-5758.

Dehghanpour, H., Lan, Q., Saeed, Y., Fei, H., & Qi, Z. (2013). Spontaneous imbibition of brine and oil in gas shales: effect of water adsorption and resulting microfractures. Energy & Fuels, 27(6), 3039-3049.

Dohmen, T., Blangy, J.P., Zhang, J., (Aug 2014). Microseismic Depletion Delineation. Interpretation, 2 (3).

Downie, R. C., le Calvez, J., Dean, B. K., & Rutledge, J. (2015, February 3). Correlation and Interpretation of Microseismic Responses Using Pressure Measurements in Offset Observation Wells. Society of Petroleum Engineers. doi:10.2118/173386-MS

Duncan, R. C., & Youngquist, W. (1999). Encircling the peak of world oil production. Natural Resources Research, 8(3), 219-232.

Economides, M.J., and Nolte, K.G., Reservoir Simulation, 3rd Ed., John Wiley, Chichester, England; New York.

Elbel, J. L., & Sookprasong, P. A. (1987, August 1). Use of Cumulative-Production Type Curves in Fracture Design. Society of Petroleum Engineers. doi:10.2118/14510-PA

Holcomb, D. J. (1993) General Theory of the Kaiser Effect. Int. J. Rock Mech. Min. Sci. & Geomech.

Huang, Jian., Reza Safari, Sunil Lakshminarayanan et al. 2014. Impact of discrete fracture network (DFN) reactivation on productive stimulated rock volume: microseismic, geomechanics and reservoir coupling. Paper presented at the 48th US Rock Mechanics / Geomechanics Symposium, Minneapolis, MN.

Hubbert, M.K., Willis, D.G. (1972, July). Mechanics of Hydraulic Fracturing. Society of Petroleum Engineers.

Manchanda, R., Sharma, M. M., & Holzhauser, S. (2014, November 1). Time-Dependent Fracture-Interference Effects in Pad Wells. Society of Petroleum Engineers. doi:10.2118/164534-PA

Makhanov, K., Habibi, A., Dehghanpour, H., & Kuru, E. (2014). Liquid uptake of gas shales: A workflow to estimate water loss during shut-in periods after fracturing operations. Journal of Unconventional Oil and Gas Resources, 7, 22-32.

McClure, M. W. (2012). Modeling and characterization of hydraulic stimulation and induced seismicity in geothermal and shale gas reservoirs (Doctoral dissertation, Stanford University).

McClure, M. W. (2013). Understanding, diagnosing, and modeling the causes of fracture network complexity in unconventional reservoirs. The Leading Edge,32(12), 1494-1500.

McClure, M., & Horne, R. N. (2013). Discrete fracture network modeling of hydraulic stimulation: Coupling flow and geomechanics. Springer Science & Business Media.

McClure, M., Babazadeh, M., Shiozawa, S., & Huang, J. (2015, February 3). Fully Coupled Hydromechanical Simulation of Hydraulic Fracturing in Three-Dimensional Discrete Fracture Networks. Society of Petroleum Engineers. doi:10.2118/173354-MS

Medeiros, F., Kurtoglu, B., Ozkan, E., & Kazemi, H. (2010, June 1). Analysis of Production Data From Hydraulically Fractured Horizontal Wells in Shale Reservoirs. Society of Petroleum Engineers. doi:10.2118/110848-PA

Montgomery, Scott L., et al. "Mississippian Barnett Shale, Fort Worth basin, north-central Texas: Gas-shale play with multi–trillion cubic foot potential."AAPG bulletin 89.2 (2005): 155-175.

Nagel, N., I. Gil, M. Sanchez-Nagel, and B. Damjanac (2011), Simulating hydraulic fracturing in real fractured rocks - overcoming the limits of pseudo3d models, SPE 140480, paper presented at the SPE Hydraulic Fracturing Technology Conference, The Woodlands, Texas, USA, doi:10.2118/140480-MS.

Palmer, I., Z. Moschovidis, and J. Cameron (2007), Modeling shear failure and stimulation of the Barnett Shale after hydraulic fracturing, SPE 106113, paper

presented at the SPE Hydraulic Fracturing Technology Conference, College Station, Texas, U.S.A., doi:10.2118/106113-MS.

Paulding, B. W. (1967, January 1). Orientation of Hydraulically Induced Fractures. American Rock Mechanics Association

Rogers, S., D. Elmo, R. Dunphy, and D. Bearinger (2010), Understanding hydraulic fracture geometry and interactions in the Horn River Basin through DFN and numerical modeling, SPE 137488, paper presented at the Canadian Unconventional Resources and International Petroleum Conference, Calgary, Alberta, Canada, doi:10.2118/137488-MS.

Roussel, N., and M. Sharma (2011), Strategies to minimize frac spacing and stimulate natural fractures in horizontal completions, SPE 146104, paper presented at the SPE Annual Technical Conference and Exhibition, Denver, Colorado, USA, doi:10.2118/146104-MS.

Vinsome, P. K., and J. Westerveld (1980), A simple method for predicting cap and base rock heat loses in thermal reservoir simulators, Journal of Canadian Petroleum Technology, 19(3), 87-90, doi:10.2118/80-03-04.

Vincent, M. C. (2012). The next opportunity to improve hydraulic-fracture stimulation. Journal of Petroleum Technology, 64(03), 118-127.

Warpinski, N. R., W. S.L, and C. A. Wright (2001), Analysis and prediction of microseismicity induced by hydraulic fracturing, SPE 71649, paper presented at the SPE Annual Technical Conference and Exhibition, New Orleans, Louisiana, oi:10.2118/71649-MS.

Warpinski, N. (2009, November 1). Microseismic Monitoring: Inside and Out. Society of Petroleum Engineers. doi:10.2118/118537-JPT

Warpinski, N. R., Mayerhofer, M., Agarwal, K., & Du, J. (2013, May 6). Hydraulic-Fracture Geomechanics and Microseismic-Source Mechanisms. Society of Petroleum Engineers. doi:10.2118/158935-PA

Warpinski, N. R., and L. W. Teufel (1987), Influence of geologic discontinuities on hydraulic fracture propagation, Journal of Petroleum Technology, 39(2), doi:10.2118/13224-PA.

Weng, X., O. Kresse, C.-E. Cohen, R. Wu, and H. Gu (2011), Modeling of hydraulic-fracture-network propagation in a naturally fractured formation, SPE Production & Operations, 26(4), doi:10.2118/140253-PA.

Wu, R., O. Kresse, X. Weng, C. Cohen, and H. Gu (2012), Modeling of interaction of hydraulic fractures in complex fracture networks, paper presented at the SPE Hydraulic Fracturing Technology Conference, The Woodlands, Texas, USA, doi:10.2118/152052-MS.